THE INFLUENCE OF ARTIFICIAL CAVITIES ON NATURAL CONVECTION HEAT TRANSFER FROM A HORIZONTAL SURFACE

Apichart Penkitti

NAVAL POSTGRADUATE SCHOOL
Monterey, California

THESIS

The Influence Of Artificial Cavities On
Natural Convection Heat Transfer
From A Horizontal Surface

by

Apichart Penkitti

December 1975

Thesis Advisor: - M. D. Kelleher

Approved for public release; distribution unlimited.

REPORT DOCUMENTATION PAGE

READ INSTRUCTIONS BEFORE COMPLETING FORM

1. REPORT NUMBER

2. GOVT ACCESSION NO.

3. RECIPIENT'S CATALOG NUMBER

4. TITLE (and Subtitle)
The Influence of Artificial Cavities On Natural Convection Heat Transfer From a Horizontal Surface

5. TYPE OF REPORT & PERIOD COVERED
Master's Thesis; December 1975

6. PERFORMING ORG. REPORT NUMBER

7. AUTHOR(s)
Apichart Penkitti

8. CONTRACT OR GRANT NUMBER(s)

9. PERFORMING ORGANIZATION NAME AND ADDRESS
Naval Postgraduate School
Monterey, CA 93940

10. PROGRAM ELEMENT, PROJECT, TASK AREA & WORK UNIT NUMBERS

11. CONTROLLING OFFICE NAME AND ADDRESS
Naval Postgraduate School
Monterey, CA 93940

12. REPORT DATE
December 1975

13. NUMBER OF PAGES
65

14. MONITORING AGENCY NAME & ADDRESS(if different from Controlling Office)
Naval Postgraduate School
Monterey, CA 93940

15. SECURITY CLASS. (of this report)
UNCLASSIFIED

15a. DECLASSIFICATION/DOWNGRADING SCHEDULE

16. DISTRIBUTION STATEMENT (of this Report)
Approved for public release; distribution unlimited.

17. DISTRIBUTION STATEMENT (of the abstract entered in Block 20, if different from Report)

18. SUPPLEMENTARY NOTES

19. KEY WORDS (Continue on reverse side if necessary and identify by block number)
Natural Convection
Horizontal Disk
Cylindrical Enclosure
Test Section

20. ABSTRACT (Continue on reverse side if necessary and identify by block number)
The objective of this project was to study the effect of small artificial cavities on natural convection from a horizontal surface. Tests were run with Freon 113. Data for heat flux as a function of bulk temperature difference were carefully obtained. These data yielded Nusselt number as a function of Grashof number or Rayleigh number. All of these were then

20. Abstract (continued)

compared with the data obtained by Hiep [Ref. 2]. Experimental results are presented for the heat transfer from horizontal circular disks, with and without artificial cavities.

The artificial cavities were found to affect the natural convection heat transfer from a horizontal surface: the heat transfer coefficients increased with the number of cavities.

The Influence Of Artificial Cavities On Natural Convection Heat Transfer From A Horizontal Surface

by

Apichart Penkitti
First Lieutenant, Royal Thai Army
B.S., Royal Thai Military Academy, 1972

Submitted in partial fulfillment of the
requirements for the degree of

MASTER OF SCIENCE IN MECHANICAL ENGINEERING

from the

NAVAL POSTGRADUATE SCHOOL
December 1975

ABSTRACT

The objective of this project was to study the effect of small artificial cavities on natural convection from a horizontal surface. Tests were run with Feron 113. Data for heat flux as a function of bulk temperature difference were carefully obtained. These data yielded Nusselt number as a function of Grashof number or Rayleigh number. All of these were then compared with the data obtained by Hiep [Ref. 2]. Experimental results are presented for the heat transfer from horizontal circular disks, with and without artificial cavities.

The artificial cavities were found to affect the natural convection heat transfer from a horizontal surface: the heat transfer coefficients increased with the number of cavities.

TABLE OF CONTENTS

I. INTRODUCTION---------- 11

A. BACKGROUND---------- 11

B. THESIS OBJECTIVES---------- 13

II. EXPERIMENTAL APPARATUS---------- 14

A. DESIGN CONSIDERATIONS---------- 14

B. TEST SECTION-HEATER ASSEMBLY---------- 14

C. INSTRUMENTATION---------- 24

1. Temperature Measurement---------- 24

2. Power to Heater---------- 25

III. EXPERIMENTAL PROCEDURE---------- 27

A. TEST SURFACE PREPARATION---------- 27

B. APPARATUS ASSEMBLY---------- 28

C. FLUID PREPARATION---------- 30

1. Temperature---------- 30

2. Determination of Nusselt, Grashof, and Rayleigh Numbers---------- 31

IV. RESULTS AND DISCUSSION---------- 33

V. CONCLUSIONS---------- 47

APPENDIX A - THERMOCOUPLE CALIBRATION PROCEDURE-------- 49

APPENDIX B - SAMPLE CALCULATIONS---------- 51

APPENDIX C - UNCERTAINTY ANALYSIS---------- 56

BIBLIOGRAPHY---------- 63

INITIAL DISTRIBUTION LIST---------- 65

LIST OF TABLES

I. Summary of Results for Blank Test Section---------- 34

II. Summary of Results for Seven-Hole Test Section----- 35

III. Summary of Results for Thirteen-Hole Test Section-- 36

IV. Uncertainty of Variables---------- 56

V. Uncertainty in Experiment for Blank Test Section--- 60

VI. Uncertainty in Experiment for Seven-Hole Test Section---------- 61

VII. Uncertainty in Experiment for Thirteen-Hole Test Section---------- 62

LIST OF FIGURES

Figure 1. Photograph of Complete Apparatus Including Instrumentation---------- 15

Figure 2. Photograph of Assembled Experimental Unit----- 16

Figure 3. Cross Section View of Tank, Test Section and Heater Assembly---------- 17

Figure 4. Photograph of Blank Test Section After the Test---------- 18

Figure 5. Photograph of Thirteen-Hole Test Section After the Test---------- 19

Figure 6. Cross Section View of Blank Test Section------ 20

Figure 7. Cross Section View of Seven-Hole Test Section- 21

Figure 8. Cross Section View of Thirteen-Hole Test Section---------- 22

Figure 9. Cross Section View of Heater Assembly--------- 23

Figure 10. Log-Log Plot of Nusselt Number vs Grashof Number for Blank Test Section---------- 39

Figure 11. Log-Log Plot of Nusselt Number vs Rayleigh Number for Blank Test Section---------- 40

Figure 12. Log-Log Plot of Nusselt Number vs Grashof Number for Seven-Hole Test Section---------- 41

Figure 13. Log-Log Plot of Nusselt Number vs Rayleigh Number for Seven-Hole Test Section---------- 42

Figure 14. Log-Log Plot of Nusselt Number vs Grashof Number for Thirteen-Hole Test Section--------- 43

Figure 15. Log-log Plot of Nusselt Number vs Rayleigh Number for Thirteen-Hole Test Section--------- 44

Figure 16. Log-Log Plot of Nusselt Number vs Grashof Number for all Data---------- 45

Figure 17. Log-Log Plot of Nusselt Number vs Rayleigh Number for all Data---------- 46

Figure 18. Determination of Surface Temperature--------- 52

NOMENCLATURE

Symbol	Description	Units
C_p	Specific Heat	BTU/lb_m-°F
D	Test Surface Diameter	Inches or ft.
g	Acceleration of Gravity	Ft/sec^2
h	Convection Heat Transfer Coefficient	BTU/Hr-Ft^2-°F
H	Height of Cylindrical Tank	Inches or ft.
K_{ss}	Thermal Conductivity of 304 Stainless Steel	BTU/Hr-Ft-°F
k_f	Thermal Conductivity of Freon 113	BTU/Hr-Ft-°F
P	Power into Heater	Watts
R	Radius of Cylindrical Tank	Inches or ft.
T_b	Bulk Temperature of Fluid	°F
T_s	Test Section Surface Temperature	°F
δT_1	Temperature Difference Between Test Surface and Fluid (T_s-T_b)	°F
T_2	Temperature Measured in Stainless Steel Test Section about 0.72 inch From Test Surface	°F
T_3	Temperature Measured in Stainless Steel Test Section About 0.22 Inch From Test Surface	°F

Symbol	Description	Units
δT_2	Temperature Difference in Test Section (T_2-T_3)	°F
T_f	Film Temperature $[\frac{T_s+T_b}{2}]$	°F
δx	Distance in Stainless Steel Test Section Between Thermocouple No. 2 and Thermocouple No. 3	Inches or ft.
$U_{subscript}$	Uncertainly in variable denoted by subscript, for example: U_{T_b} is uncertainty in T_b	Units of variable denoted by subscript
α	Fluid Coefficient of	Ft^2/sec
β	Fluid Coefficient of Thermal Expansion	$\frac{1}{°F}$
μ	Fluid Dynamic Viscosity	$lb_m/hr\text{-}ft$
ν	Fluid Kinematic Viscosity	Ft^2/sec
ρ	Fluid Density	lb_m/ft^3
Dimensionless Numbers		
Nu	Nusselt Number Based on Test Section Surface Diameter	hD/k_f
Pr	Fluid Prandtl Number	$\frac{\mu Cp}{k_f}$, $\frac{\nu}{\alpha}$
Gr	Grashof Number Based on Test Section Surface Diameter	$\frac{g\beta D^3\ \delta T_1}{\nu^2}$
Ra	Rayleigh Number	Gr.Pr

ACKNOWLEDGMENT

The author wishes to thank Professor M.D. Kelleher, his thesis advisor, for his advice and assistance in this work. Without his guidance this work could not have been completed.

He wishes to express his gratitude to Professor Paul Marto, Professor Thomas Cooper for their advice and all of the Mechanical Engineering Department for their advice and work on the design of the experimental apparatus.

A special word of thanks and sincere appreciation to my wife, Phontip, without whose understanding and patience, the entire undertaking would have been extremely difficult.

I. INTRODUCTION

A. BACKGROUND

It has been shown by Duncan [Ref. 1] that artificial cavities can have a significant effect on boiling heat transfer. If the cavities are of the correct size it is possible to induce nucleation at lower superheats than would otherwise be necessary. Recognizing the enhanced heat transfer which artificial cavities can induce in the boiling regime one is led to inquire as to the effect that these cavities might have on the natural convection heat transfer which precedes boiling. Hiep [Ref. 2] undertook an experimental investigation of the effect of artificial cavities on the natural convection heat transfer from a horizontal circular disc. Tests were run with water and Freon 113. For water O'Connor [Ref. 3] ran tests with a mirror finished test surface without the artificial cavities and plotted the data in terms of dimensionless parameters, Nusselt number versus Grashof number. Hiep started with seven artificial cavities for water, and gave the correlation result of Nusselt number in term of Rayleigh number as:

$$Nu = 0.38\ (Ra)^{0.29} \qquad (1)$$

For Freon 113 Hiep ran the tests with a blank and seven-hole test sections, again he gave the results in terms of Nusselt number versus Grashof number and Nusselt number against

Rayleigh number the correlation results for blank test section was

$$Nu = 0.48\ (Ra)^{0.30} \qquad (2)$$

The experimental apparatus that O'Connor [Ref. 3] and Hiep [Ref. 2] used was almost the same. Test surface had a diameter of 0.895 inches, installed in the center of a cylindrical tank 9.00 inches in diameter and 4.5 inches high and set at the same level as the tank floor (see Figure 3). A controllable resistance heater as a heat source was housed in a copper block attached to the bottom of test section. A calibrated resistor in series with the heater was used to determine accurately the input power to the heater. Eight thermocouples, wired in series were used to measure the average bulk temperature of the fluid and one removable thermocouple was used to provide a check on this temperature. To record the temperature distribution in the stainless steel cylinder, four stainless steel sheathed thermocouples were equally spaced along the axis of the test section. The temperatures at these locations were obtained using a Dana digital voltmeter.

Since all the results and discussion of Hiep's work depend on the accuracy of determination of the test surface and fluid temperature the calibration of all thermocouples is extremely important. Hiep used the standard thermocouple tables instead of the average of his calibration value. The

uncertainty value in Hiep's thermocouple reading was 0.5°F, which results in a large uncertainty for heat transfer coefficient. The change in Nusselt number between the blank test section and the seven hole test section as determined by Hiep is within the experimental uncertainty assigned to the Nusselt number.

The uncertainty in Hiep's experimental data, therefore, tends to make it difficult to draw a firm conclusion as to the effect which artificial cavities have on the natural convection heat transfer process. His experiments were limited to two test surfaces, blank and seven cavities. He also limited the range of surface temperature to those below the saturation temperature of Freon 113. In other words the experiment did not go into the boiling phase that Duncan [Ref. 1] obtained.

B. THESIS OBJECTIVES

The previous discussion has led to the objection of this experimental works, that is:

1. To investigate the effects of the drilled cavities on natural convection heat transfer in Freon 113 with greater number of test surfaces than Hiep obtained.
2. To obtain results for the boiling phase of Freon 113 to see if it agrees with the Duncan results.
3. Try to keep the uncertainty value of heat transfer coefficient and other dimensionless parameters as low as possible.

II. EXPERIMENTAL APPARATUS

A. DESIGN CONSIDERATION

1. The experimental apparatus used in this study is the same as had been used by Hiep [Ref. 1]. A complete description can be found in his thesis and the thesis of O'Conner [Ref. 3]. A schematic diagram of the experimental set-up is shown in Figure 3. For convenience the ice-bath used by Hiep was replaced by an automatic electronic ice-point for the reference thermocouple. This automatic ice junction was set to 32°F as reference temperature. A Dana digital voltmeter that had been used to read and record the thermocouples was replaced by a Hewlett Packard digital voltmeter.

2. A Freon condenser was also added to recover the Freon that evaporates during the experiment. This condenser was connected to the top plate of the tank as shown in Figure 2, and was cooled by tap water.

B. TEST SECTION-HEATER ASSEMBLY

Three test sections were used in this experimental work: one blank, one with seven holes which had been used by Hiep and one with thirteen holes (cylindrical drilled cavities). All three test surfaces had the same diameter, that is .896 inch. Four 0.040 inch diameter holes were drilled along the length of each test piece to a depth of 0.375 inches, separated axially by about 0.5 inch and 90° apart from each other. These holes were for sheathed thermocouples installation in

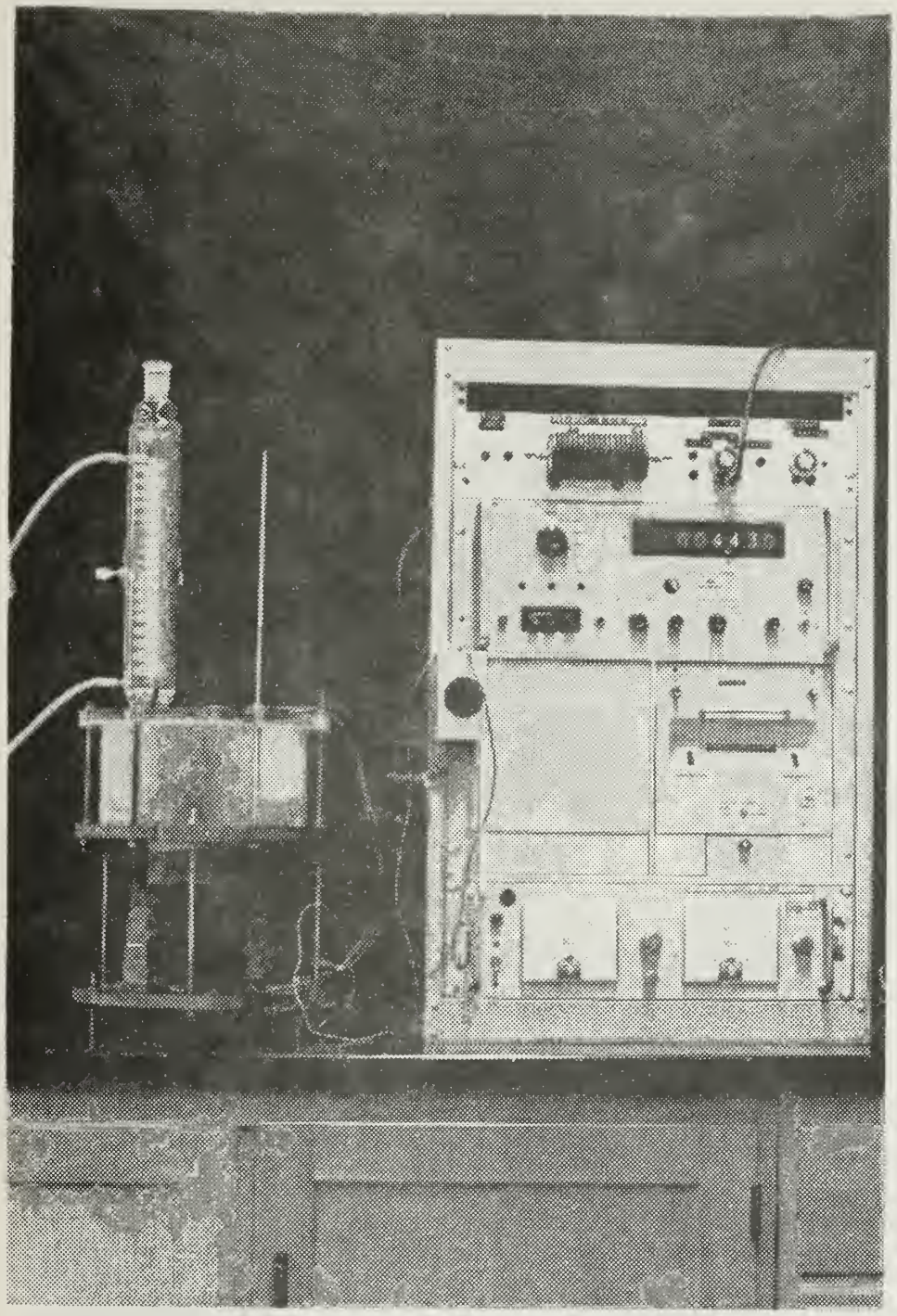

Figure 1. Photograph of Complete Apparatus Including Instrumentation.

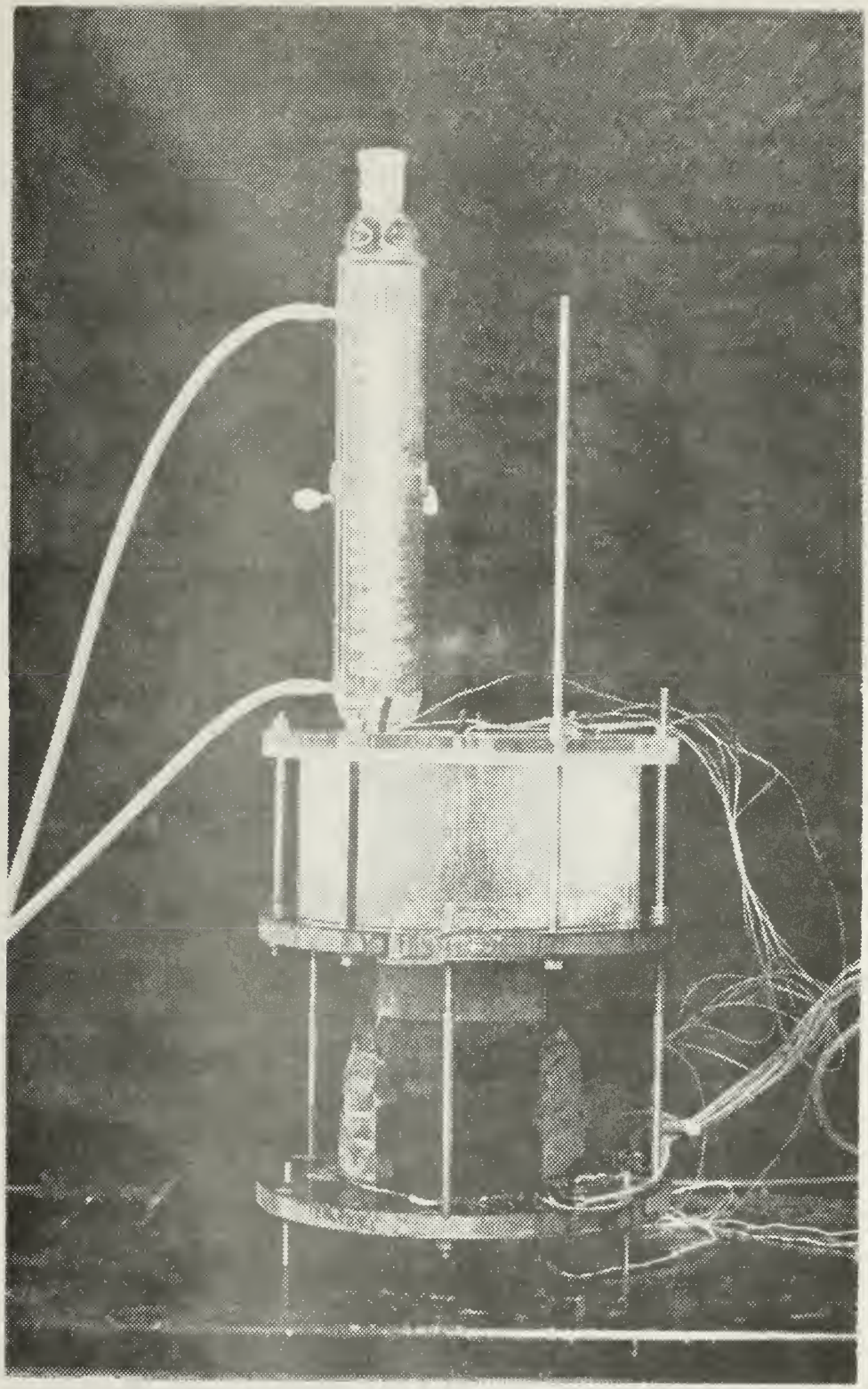

Figure 2. Photograph of Assembled Experimental Unit.

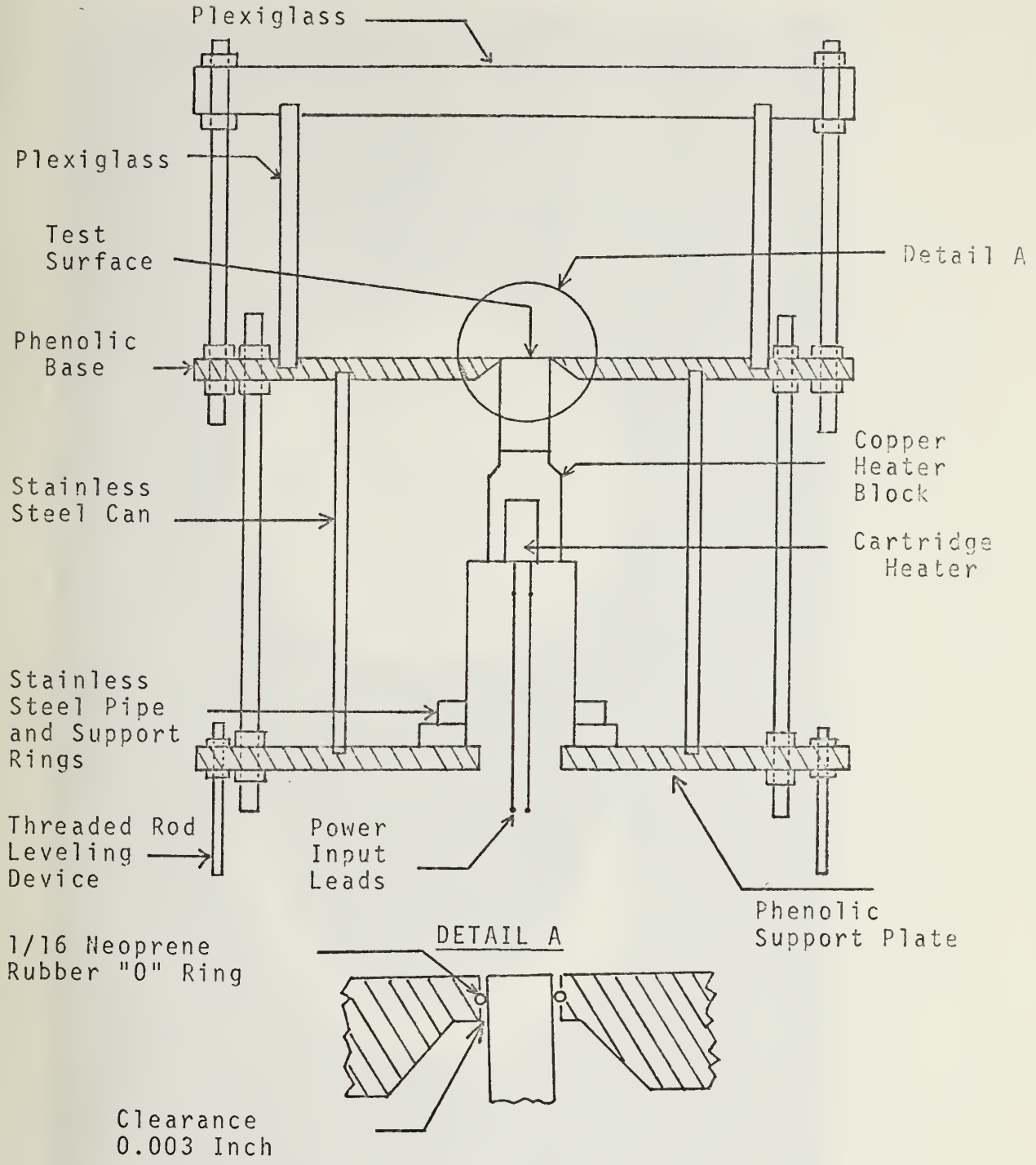

Figure 3. Cross Sectional View of Tank, Test Section and Heater Assembly.

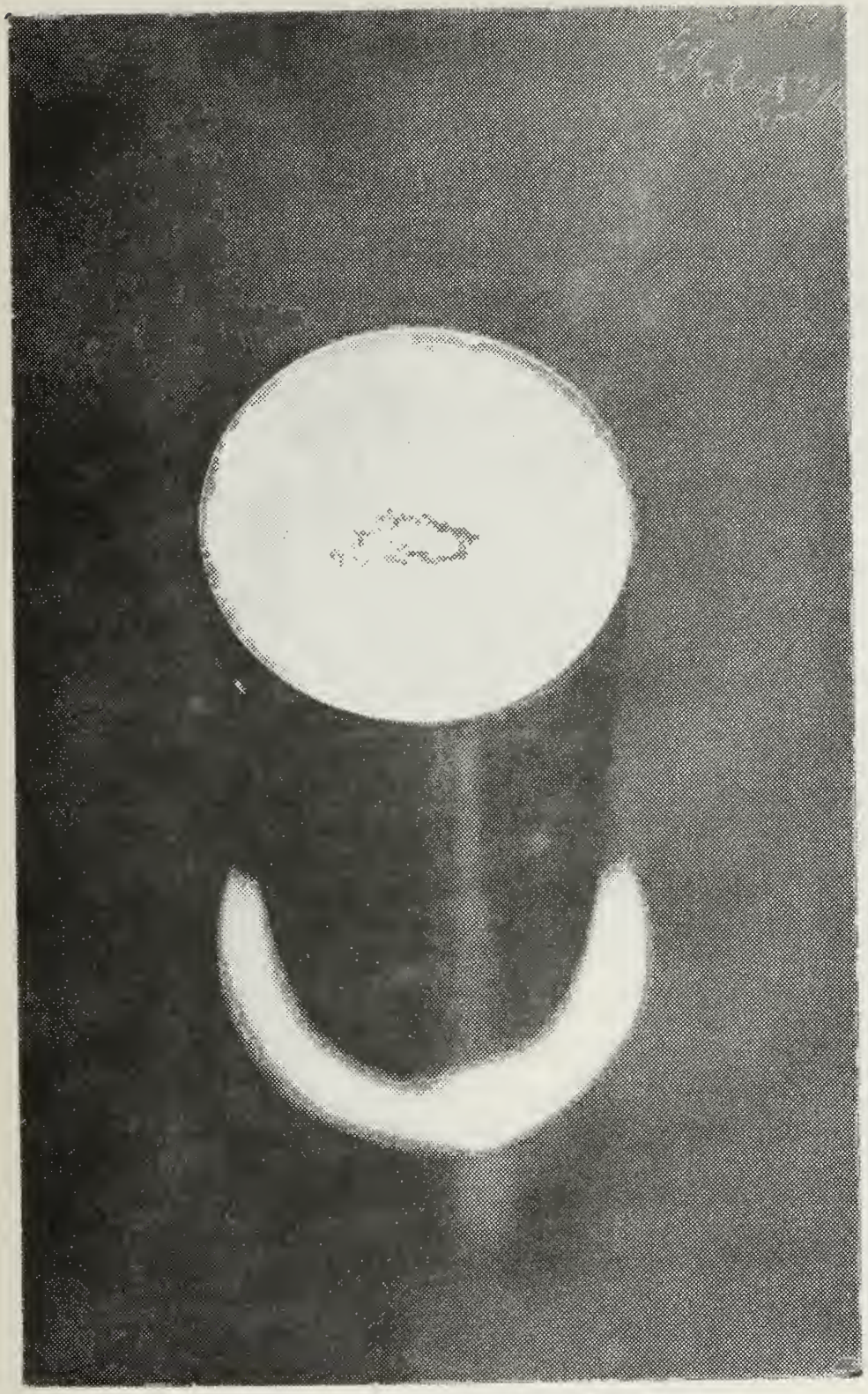

Figure 4. Photograph of Blank Test Section After the Test.

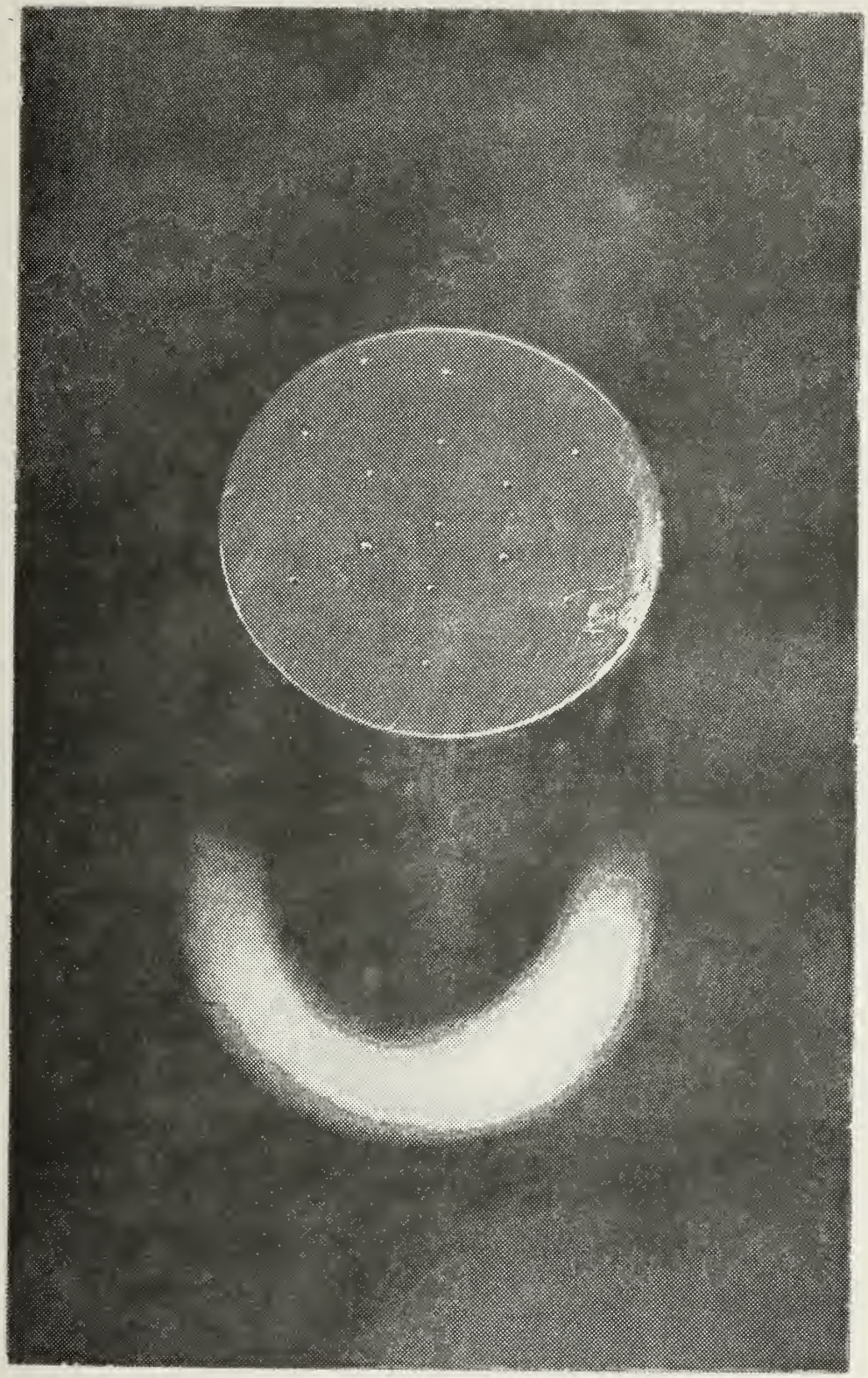

Figure 5. Photograph of Thirteen-Hole Test Section After the Test.

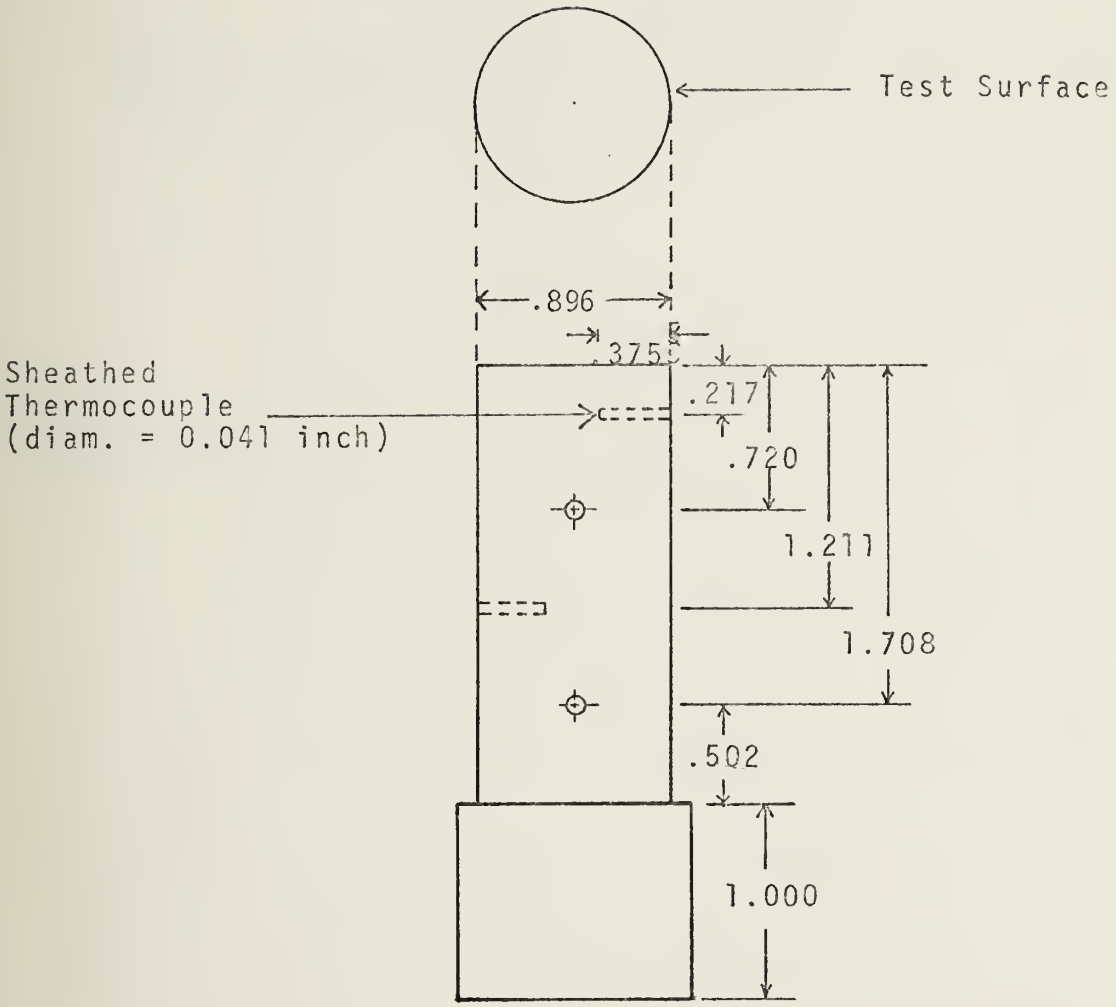

Figure 6. Blank Test Section.

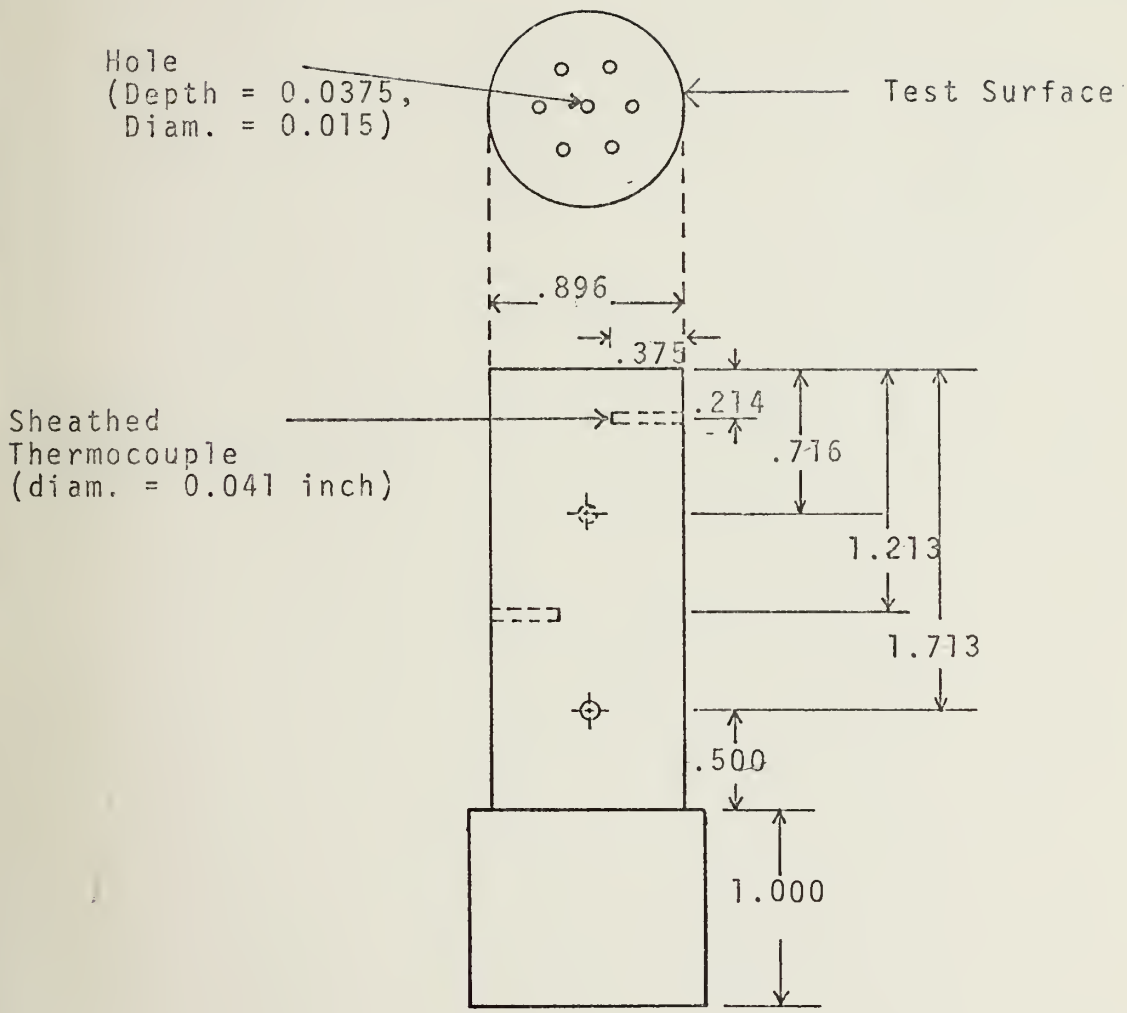

Figure 7. Seven-Hole Test Section.

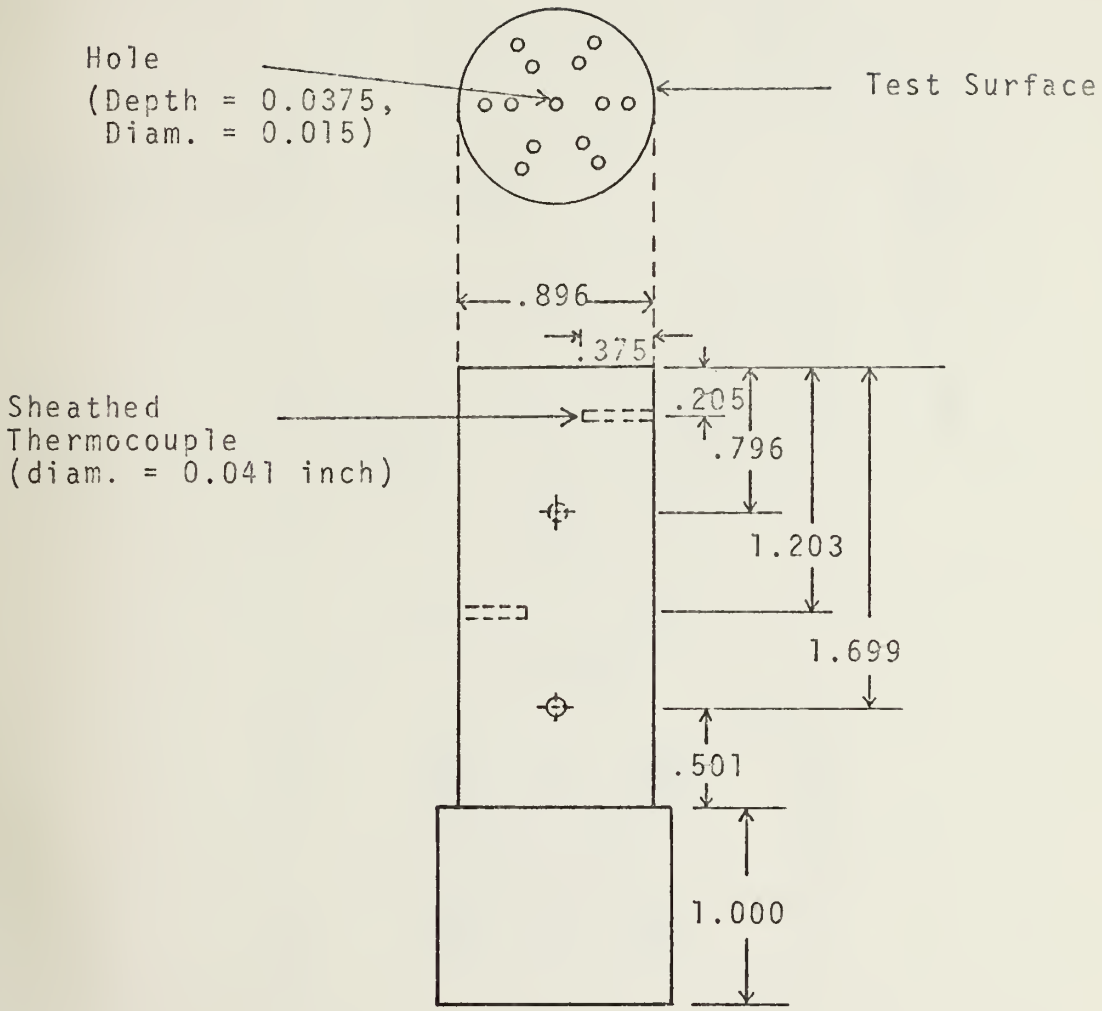

Figure 8. Thirteen-Hole Test Section.

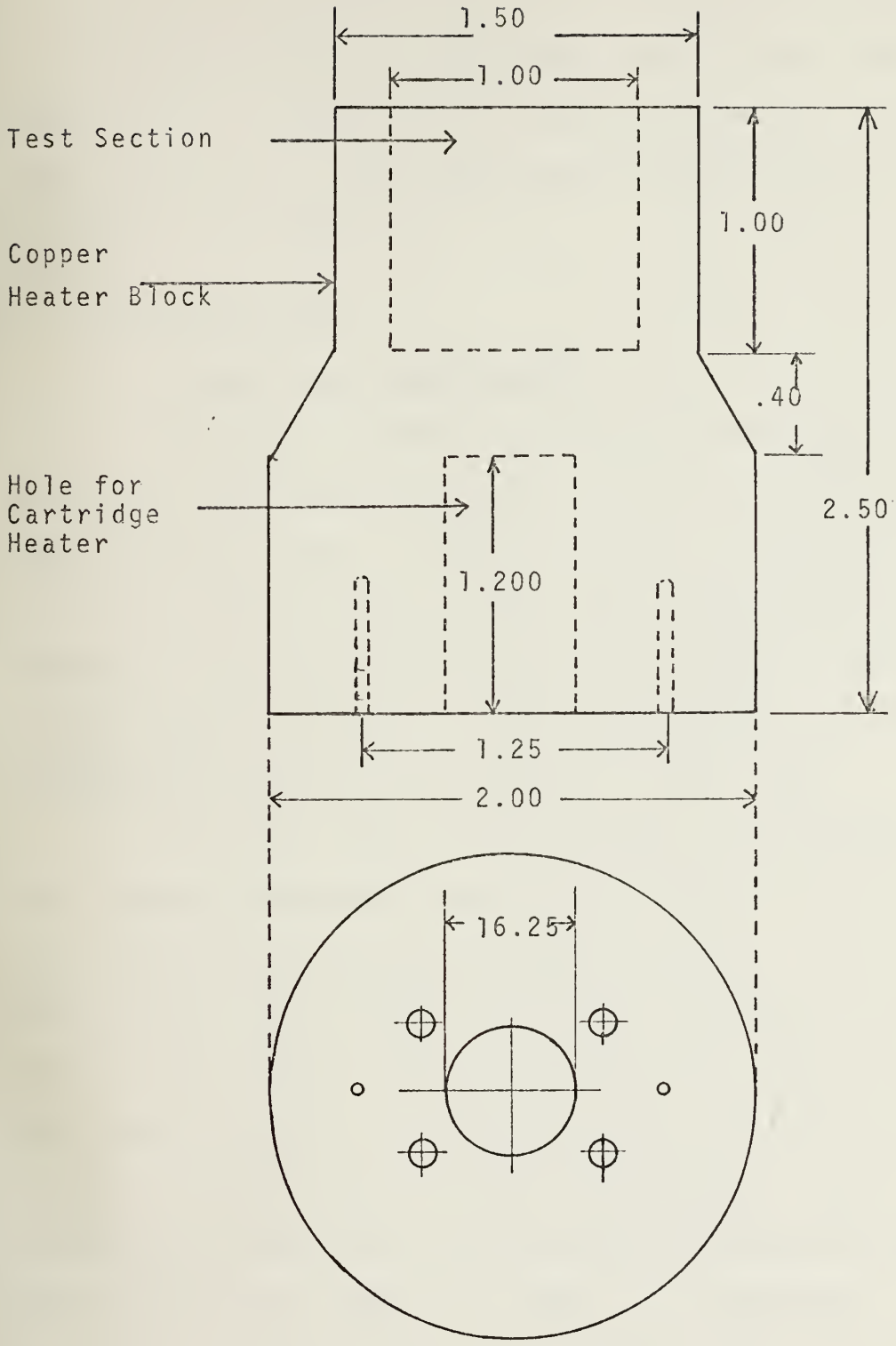

Figure 9. Heater Assembly.

each test section as shown in Figure 6-8. The thirteen-hole test section had thirteen cylindrical holes of the same size as the holes drilled on seven-hole test section, that is 0.0375 inch in depth and 0.015 inch in diameter, drilled as shown in Figure 8. The heater section [Fig. 9] was the same as used by Hiep [Ref. 2].

C. INSTRUMENTATION

1. Temperature Measurement

ISA type T copper-constantan thermocouples were used to measure the temperature distribution in stainless steel test section in order to get as accurate as possible in temperature distribution. These four thermocouples were sheathed in stainless steel (sheathed diameter = 0.035 inch) and the temperature of the surface was found by using a linear extrapolating method (see Appendix II, Fig. 18).

The bulk fluid temperature was determined by using eight copper-constantan thermocouples wired in series (four pairs) manufactured using a Dynatech welder. These thermocouples were wired in series into an insulated switching box so the reading gave an average temperature for four pairs of these thermocouples. A single removable thermocouple was used to provide a check on this temperature. The sheathed thermocouple leads were securely fastened to the bottom phenolic plate and then to a Jones bar arrangement. Because the sheathed thermocouples were difficult to manipulate and subject to twisting, and thus shorting, giving erroneous

reading, the more flexible wires were used for the bulk temperature thermocouples were used as extension wire into the switching box. A reference thermocouple was inserted into the automatic ice-point reference. A Hewlett Packard digital voltmeter accurate to 0.001 millivolt was used to read the output of the thermocouple in millivolt.

2. Power to Heater

A Lambda regulated power supply was used to provide input voltage to the heater. A calibrated resistor was placed in series with the power supply and heater. This resistor was mounted on a large heat sink and was isothermal and therefore of constant resistance for all of the experimental runs. With this arrangement, a voltage reading across the resistor and across the heater were recorded. Knowing the voltage, and resistance, the current through the circuit could be determined by Kirchoff current law:

$$I_H = I_R = V_{R/}R \qquad (3)$$

where I_H = the current across the heater.

I_R = the current across the resistor.

R = 2.013 ohm.

V_R = voltage across the resistor.

and the product of this current and voltage across the heater gave the input power, i.e.,

$$P = V_H I_H$$

or

$$P = V_H(V_{R/}R) \quad \text{watts.} \qquad (4)$$

This value could be accurately reset for different runs. The voltage across the heater and across the calibrated resistor were determined using the Hewlett-Packard digital voltmeter, with an accuracy of 0.001 volts. This power was not used to determined the heat flux but only to set the operating point from run to run.

III. EXPERIMENTAL PROCEDURE

A. TEST SURFACE PREPARATION

It was very important that the test surface be free from any machine marks and scratches that could influence the heat transfer other than the artificial holes. For this reason the surface was mirror finished. The machine marks were removed by using a Buehler Metallurgical Manual grinder; both 0 emery polishing paper and 3/0 emery polishing paper were used. After that, the surface was washed with detergent and warm water to remove the previous abrasive and then washed with alcohol. In order to get a mirror finish the test surface was then wet polished on a metallurgical wheel covered with velvet. The wheel was impregnated with one micron diamond dust. The test surface was placed face down on the wheel and a low speed of rotation was used. During this work alcohol was used to wet the surface at all times. After completion of polishing, the test surface was washed with alcohol again and was dried with a dryer, and then wrapped with special paper to prevent contamination and touching. Before installation the seven-hole and thirteen-hole test sections were put in an ultrasonic cleaner for ten minutes, were washed with distilled water, rinsed with acetone and dried.

The seven-hole and thirteen-hole test surfaces were drilled before the mirror finish, by using a Sphinx spirec pivot drill, 0.015 inch diameter. The cavities depth were

controlled by using a feeler gauge on the lathe. A ratio of approximately 2.5 was desired for cavity depth to diameter, so the depth was about 0.040 inch; the location of seven holes and thirteen holes were as shown in Figures 7 and 8 respectively.

A height gauge which had a scale readable up to 0.0001 inch was used to determine the location of the center of the thermocouple holes relative to the test surface. This gauge was also used to measure the diameter of the test surface.

B. APPARATUS ASSEMBLY

The main parts of the apparatus were the test section, heater assembly, and the tank assembly. The test section-heater assembly was securely bolted to the phenolic base plate, as described by Heip [Ref. 2] and once the insulation was in place and the can installed, the phenolic plate that served as the bottom of the tank was carefully fitted to the test section. The level of the test section was adjusted from the bottom base of the assembly by screws. The phenolic bottom plate of the tank was secured by three threaded rods 120° apart, with the phenolic base plate. These three rods were also used to adjust the test surface in level with the phenolic bottom plate. For the tank assembly four "O" rings of 9.0 inch diameter were used for sealing to make sure that the cylindrical enclosure tank was leak proof. Two "O" rings for each side (top and bottom) of the tank were used. The

cylindrical plexiglass container was then put in place and the top installed, six threaded rods, 60° apart were used to secure the top plate to the bottom plate of the tank. The glass laboratory condenser was installed on top of the test tank to recover any vaporized Freon. Two of the threaded rods were 18 inches long so they could be used to hold the condenser and insure that it would sit tightly on the 1 inch hole at the top plate of the tank. This 1 inch hole was used to pour the fluid into or out of the tank. To hold the condenser an adjustable holder was connected from each of the 18 inch rods to make the condenser stand still. The condenser was held tightly on the top but was also removable to allow filling of the tank.

Six small holes were drilled through the plexiglass top of the tank to insert four pairs of thermocouples in the tank to measure the average bulk temperature of the fluid, for each pair one of the thermocouples was put near the bottom of the tank and the other one was placed near the top so that the average of fluid temperature all over the tank could be measured. Two holes, one in the middle of top plate and the other on the side of top plate, were used to insert one removable thermocouple to the middle of the tank to provide a check of the bulk temperature read by the other four pairs.

C. TEST PROCEDURE

1. Temperature

A complete data run consisted of starting at the lowest heater setting, waiting until steady state was reached (usually about ten hours for each data point). The data was recorded every hour during the daytime, and at longer intervals during the night. After steady state was reached and the data for that power setting was recorded, the power to the heater was increased by approximately 5 watts. This procedure was repeated until boiling occurred from the surface. The power was then decreased in 5 watt increments and the data was recorded after steady state was reached. This procedure was repeated until the starting point was reached. The procedure of taking data during both a heating and cooling process was done to check on any hysteresis effects which might exist.

The data recorded for each setting were the bulk temperature, the temperature of the individual sheathed thermocouples in the test section, and the voltages across heater and calibrated resistor. When the bulk temperature and the temperature of the test section changed by less than half degree F per hour, steady state was assumed to be reached.

2. Determination of Nusselt, Grashof and Rayleigh Numbers

For each run, at all input settings, the temperature distribution in the stainless steel test section are plotted and found to be linear. The surface temperature could be determined within 0.5°F from the plot of temperature versus thermocouple location by extrapolation, as shown in Appendix B. The properties of the fluid were determined at the film temperature which is the average of the bulk temperature (T_b) and the test surface temperature (T_S) i.e.,

$$T_f = \frac{T_b + T_S}{2}$$

The thermal conductivity of 304 stainless steel (K_{SS}) was calculated using the data from Touloukian [Ref. 10] at the average of the temperature of the two nearest thermocouples to the test surface i.e.,

$$T_{SS} = \frac{T_2 + T_3}{2} .$$

This corresponds to the average temperature of the length δx. A simple energy balance at the surface using Fourier's Law of Cooling gives:

$$K_{SS} \frac{\delta T_2}{\delta x} = h(T_S - T_b) = h\delta T_1$$

$$h = \frac{K_{SS} \cdot \delta T_2}{\delta x \cdot (\delta T_1)} \quad BTU/hr\text{-}ft^2\text{-}°F \qquad (5)$$

The Nusselt number was obtained from the definition:

$$Nu = \frac{hD}{k_f} \tag{6}$$

Substituting values of h from (3) into (4) gives:

$$Nu = \frac{K_{SS} \cdot \delta T_2 \cdot D}{\delta x \cdot (\delta T_1) \cdot k_f} \tag{7}$$

The Grashof number was calculated using the diameter of the test surface as the characteristic length:

$$Gr = \frac{g\beta D^3 (T_S - T_b)}{\nu^2} \tag{8}$$

The Rayleigh number is the product of the Grashof number and Prandlt number:

$$Ra = Gr \cdot Pr \tag{9}$$

where

$$Pr \triangleq \frac{\alpha}{\nu} = \frac{\mu Cp}{k_f} \tag{10}$$

IV. RESULTS AND DISCUSSION

It was found that a minimum of ten hours was necessary for any input setting to reach steady state. Once steady state was reached, very good agreement between Nusselt number, Grashof number and Rayleigh number, based on test surface diameter, obtained during the heating and cooling phase of the run resulted. The uncertainty bands are shown on the plot of each curve. The investigation for the blank test section covers a range of Rayleigh number from 30×10^6 to 350×10^6, for seven-hole test section from 50×10^6 to 250×10^6 and 25×10^6 to 350×10^6 for thirteen-hole test section. A summary of the results for various data runs are shown in Tables I, II, and III. For each data run the Prandtl number, Nusselt number, Grashof number and Rayleigh number were calculated. These dimensionless parameters were determined using the test section surface diameter as the characteristic length. As described in the experimental procedure, data were taken at each setting as the apparatus was heated with increasing input and then again as the inputs were decreased, cooling the test surface. The cooling phase data are denoted in the table.

Surface temperature of the test section was determined by linear extrapolation from all four sheathed thermocouple reading. This gave the surface temperature with an error of approximately .5°F.

TABLE I

Summary of Results for Blank Test Section

Input (Watt)	T_S	T_b	Nu	Log (Nu)	$Grx10^{-6}$	Log (Gr)	$Rax10^{-6}$	Log (Ra)
1.167	84.4	77.9	90.175	1.955	3.738	6.573	31.29	7.495
3.140	92.4	78.0	110.10	2.042	8.239	6.916	67.76	7.831
4.503	100.5	81.0	121.194	2.084	12.64	7.101	101.4	8.006
7.640	114.8	83.6	138.044	2.140	22.91	7.360	175.62	8.245
8.44	118.6	84.9	141.51	2.150	24.514	7.389	185.72	8.269
9.536	122.2	86.91	154.25	2.188	27.67	7.442	207.42	8.317
11.33	126.4	88.0	172.73	2.237	31.055	7.492	230.23	8.362
24.50	144.8	102.2	387.75	2.588	42.152	7.625	291.11	8.464
29.655	149.0	105.1	473.20	2.675	47.64	7.678	325.0	8.511
34.735	154.5	109.0	539.83	2.732	52.015	7.716	347.64	8.541
11.356*	126.6	86.3	169.133	2.228	32.03	7.506	238.07	8.377
9.72*	121.8	83.6	144.906	2.161	29.13	7.464	220.0	8.342
4.49*	102.0	81.7	120.40	2.081	13.14	7.119	104.65	8.020
3.234*	93.3	78.1	111.876	2.049	8.974	6.953	73.59	7.867
1.168*	85.3	78.9	88.359	1.946	3.620	6.559	30.18	7.480

Note: *represented the cooling phase.

TABLE II

Summary of Results for Seven-Hole Test Section

Input (Watt)	T_S	T_b	N_u	Log (Nu)	$Grx10^{-6}$	Log (Gr)	$Rax10^{-6}$	Log (Ra)
2.429	88.1	77.0	105.80	2.025	6.233	6.795	51.87	7.715
5.30	100.8	79.4	131.665	2.1200	13.520	7.131	108.60	8.036
7.791	113.6	84.3	146.76	2.167	21.410	7.331	164.40	8.216
10.06	121.8	86.0	159.05	2.202	26.750	7.427	201.1	8.303
14.97	130.85	91.1	231.66	2.365	33.660	7.527	245.5	8.39
10.141*	122.8	87.4	164.07	2.215	27.920	7.446	208.8	8.32
7.796*	114.0	84.6	149.72	2.175	21.400	7.331	163.9	8.215
5.299*	103.5	81.9	136.497	2.135	13.780	7.139	109.29	8.039
2.425*	90.0	79.0	110.55	2.044	6.240	6.795	51.5	7.712

Note: * represented the cooling phase.

TABLE III

Summary of Results for Thirteen-Hole Test Section

Input (Watt)	T_S	T_b	Nu	Log (Nu)	$Grx10^{-6}$	Log (Gr)	$Rax10^{-6}$	Log (Ra)
1.167	82.4	77.1	96.232	1.983	2.910	6.464	24.50	7.389
3.382	93.8	79.4	129.597	2.113	8.817	6.945	72.02	7.857
5.758	106.1	83.2	151.350	2.180	15.650	7.194	122.90	8.089
9.176	117.2	83.3	167.283	2.224	24.260	7.385	185.30	8.268
16.30	130.2	91.3	277.840	2.444	32.850	7.517	239.77	8.380
26.28	143.5	103.1	466.80	2.670	42.060	7.624	290.60	8.463
34.85	150.4	110.3	643.059	2.808	45.180	7.655	303.70	8.482
26.29*	142.9	100.5	438.504	2.642	40.970	7.612	284.70	8.454
16.41*	132.5	95.7	304.556	2.484	33.447	7.524	240.60	8.381
9.29*	119.2	86.7	180.374	2.256	24.995	7.398	188.60	8.276
5.78*	103.8	81.2	154.366	2.189	14.550	7.163	115.31	8.062
3.34*	94.4	80.1	135.440	2.132	8.870	6.948	72.20	7.859
1.528*	88.3	80.6	110.09	2.042	4.368	6.640	36.00	7.557

Note: * represented the cooling phase.

A log-log plot of Nusselt number versus Grashof number and Rayleigh number based on test surface diameter is shown for each test surface in Figures 10 to 17. The curves show that the results fall into two regimes:

1. Natural convection which is the purpose of this investigation. The Rayleigh number for this range falls in between 30×10^6 to 180×10^6 for these three test surface results. The curves show the straight line and almost have the same slope (see Figures 16 and 17). The correlation which results for the natural convection range of each test surface with Freon 113 as the fluid are:

$Nu = 0.48(Ra)^{0.30}$ $30 \times 10^6 < Ra < 180 \times 10^6$ for blank test section.

$Nu = 0.53(Ra)^{0.30}$ $30 \times 10^6 < Ra < 180 \times 10^6$ for seven-hole test section.

$Nu = 0.57(Ra)^{0.30}$ $30 \times 10^6 < Ra < 180 \times 10^6$ for thirteen-hole test section.

2. Boiling phase, the results of which must be considered with some caution. This is because the bulk temperature of the fluid was always below saturation and therefore the boiling was highly sub-cooled. In addition when nucleation occurred it began at the edge of the test surface in the space between the test section and the phenolic plate. Subsequently nucleation did take place on the test surface as can be seen by the cavitation damage visible in Figures 4 and 5. The Rayleigh number for this range started from 200×10^6 and up. The curve in this boiling phase is shown as

a straight line with slope greater than the natural convection line (also see Figure 16 and 17).

In the natural convection range the results show that the heat transfer coefficient of the fluid increases. This is consistant with Duncan's result but disagrees with Hiep's. Hiep stated that as the number of drilled cavities increase the heat transfer coefficient decrease. The discrepancy with Hiep's result can be attributed to several factors:

1. The uncertainty in thermocouple calibration which Hiep used was 0.5°F which led to a large uncertainty value in surrace temperature. Surface temperature was determined by linear extrapolation from two sheathed thermocouples near the surface. This has a large effect on the results which depend on the surface temperature. For the present experiment the value of the uncertainty in thermocouple calibration was reduced by carefully calibrating the thermocouples and using the average value of the calibration. This reduced the uncertainty in the thermocouple measurement to 0.2°F, which results in a smaller error in heat transfer coefficient.

2. The number of test surfaces that Hiep used (blank and seven-hole) was insufficient to conclude that heat transfer coefficient decreases while the number of cavities increases. That is Hiep's results for the seven-hole test section fell within the uncertainty band of the blank test section. The present experimental work used a thirteen-hole test section in addition to the seven-hole test section. These results show a consistent trend of increasing Nusselt number with increasing number of cavities.

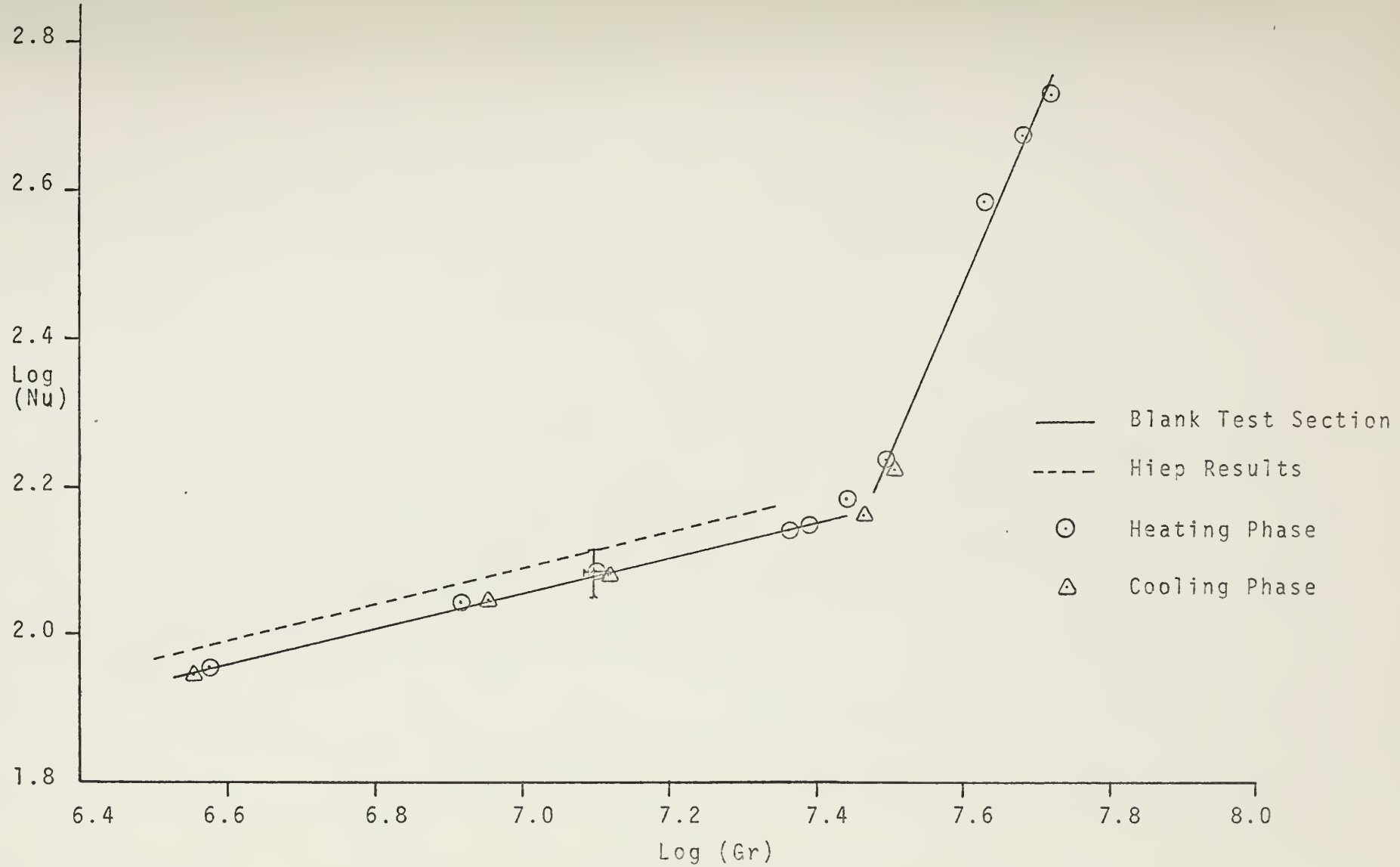

Figure 10. Results for Blank Test Section Based on Grashof Number.

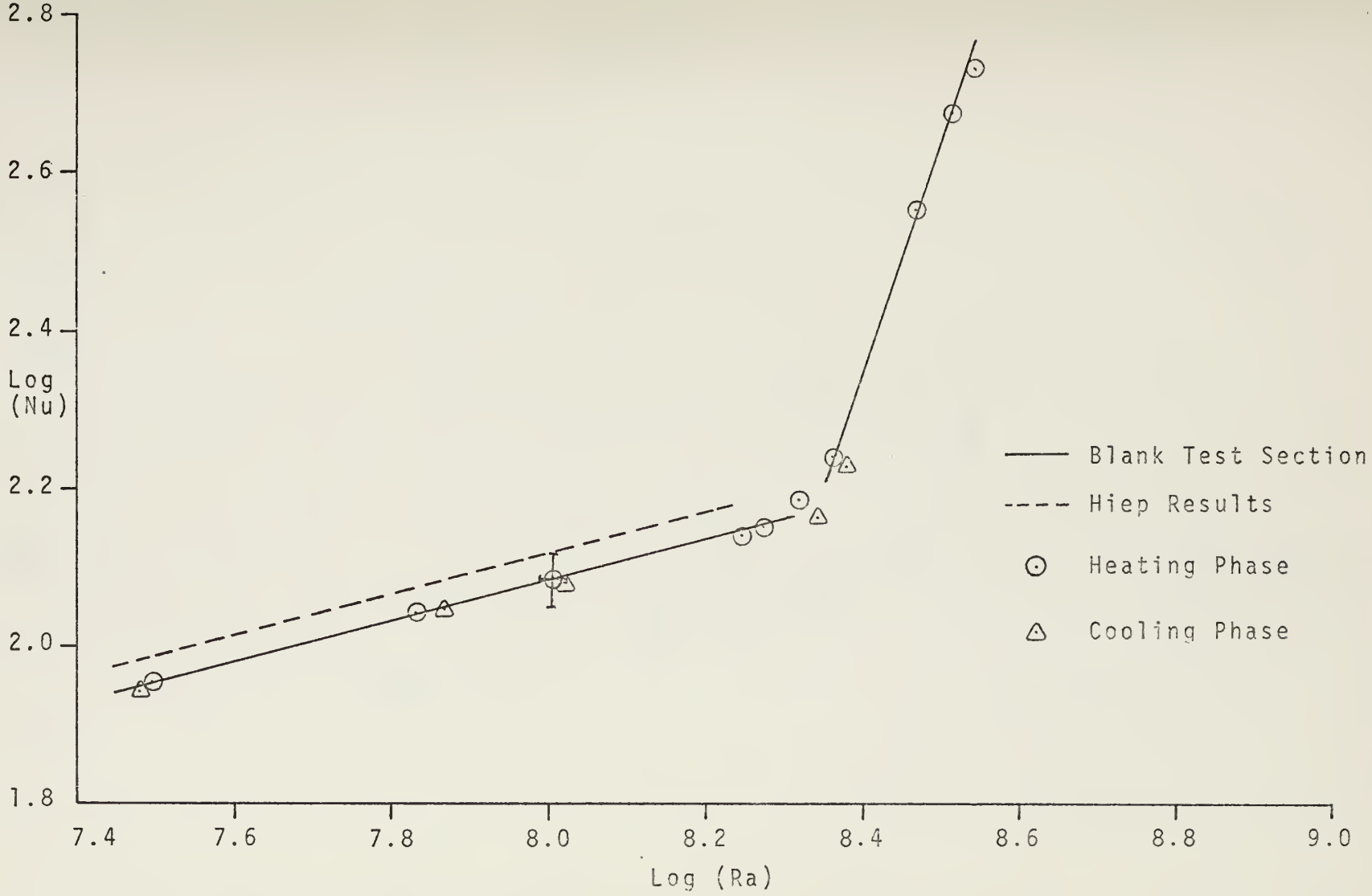

Figure 11. Results for Blank Test Section Based on Rayleigh Number.

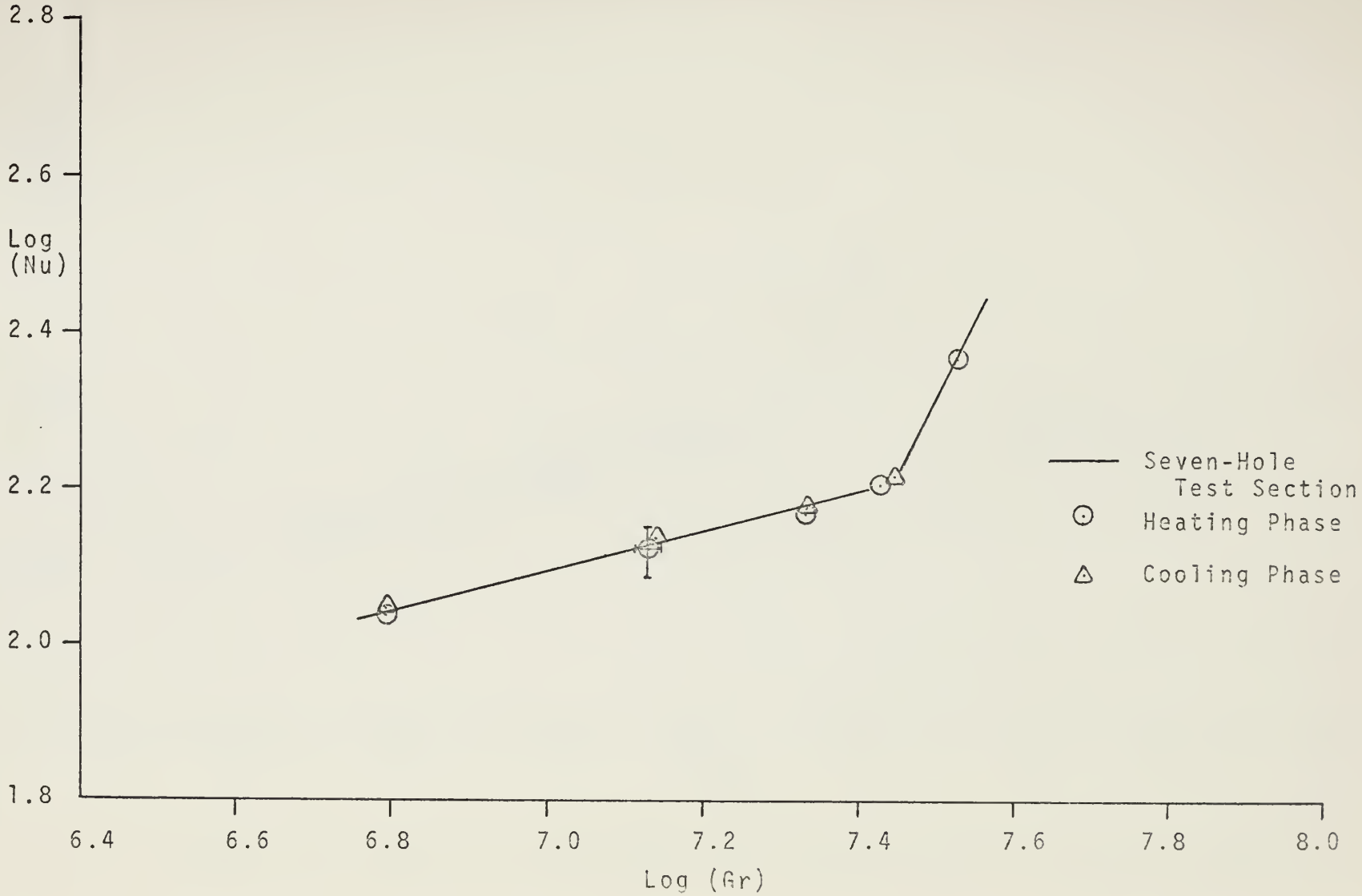

Figure 12. Results for Seven-Hole Test Section Based on Grashof Number.

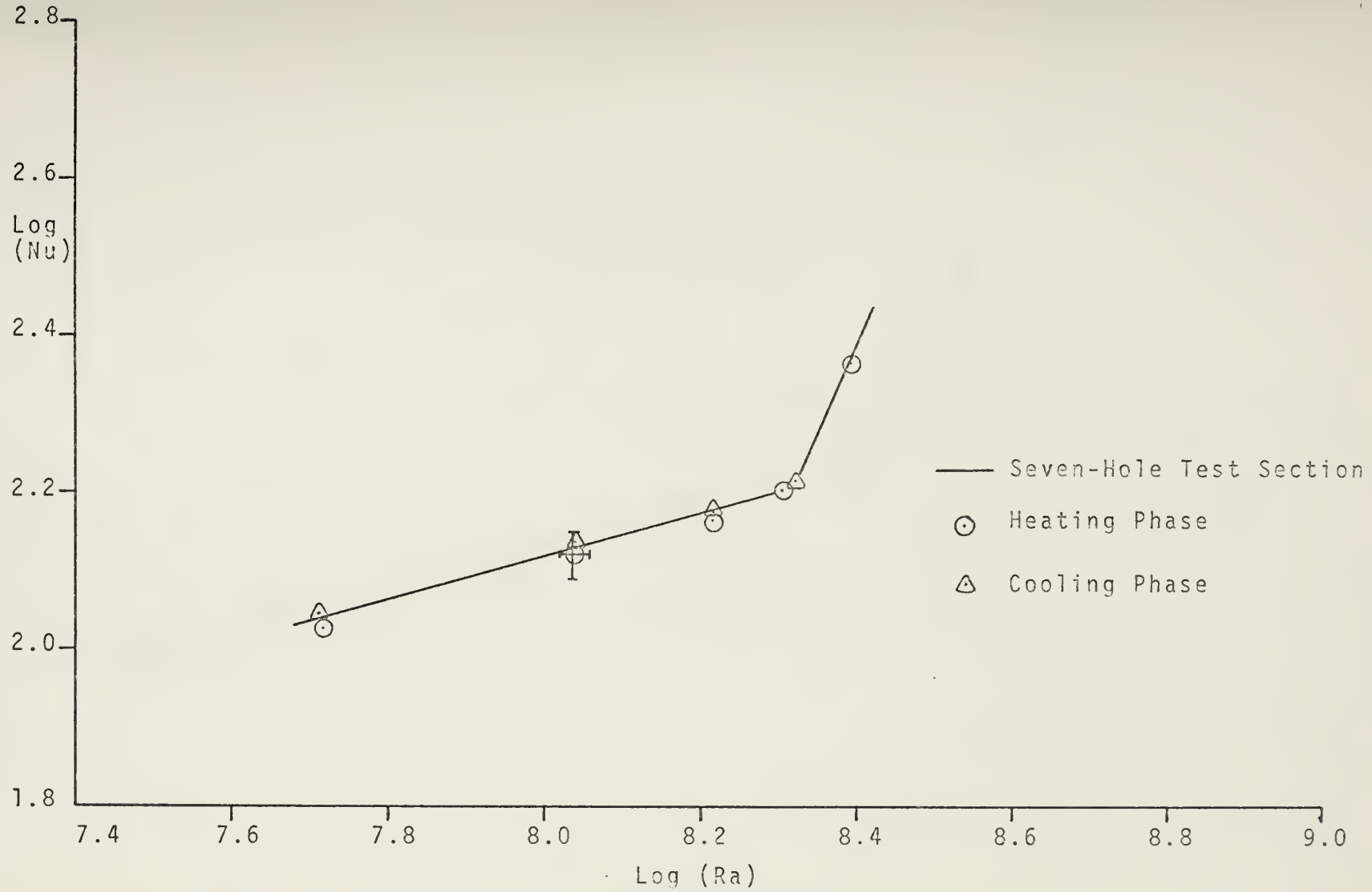

Figure 13. Results for Seven-Hole Test Section Based on Rayleigh Number.

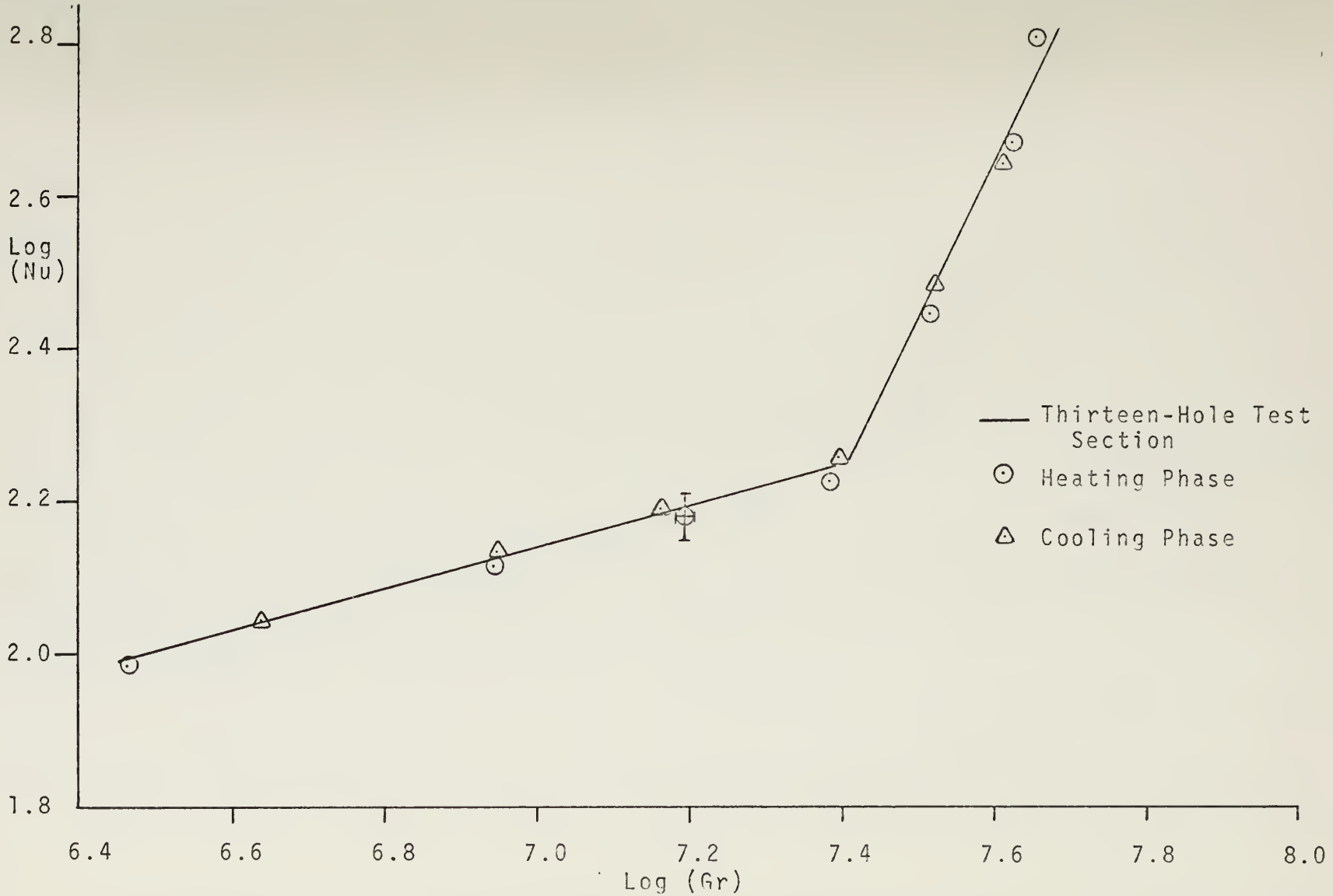

Figure 14. Results for Thirteeen-Hole Test Section Based on Grashof Number.

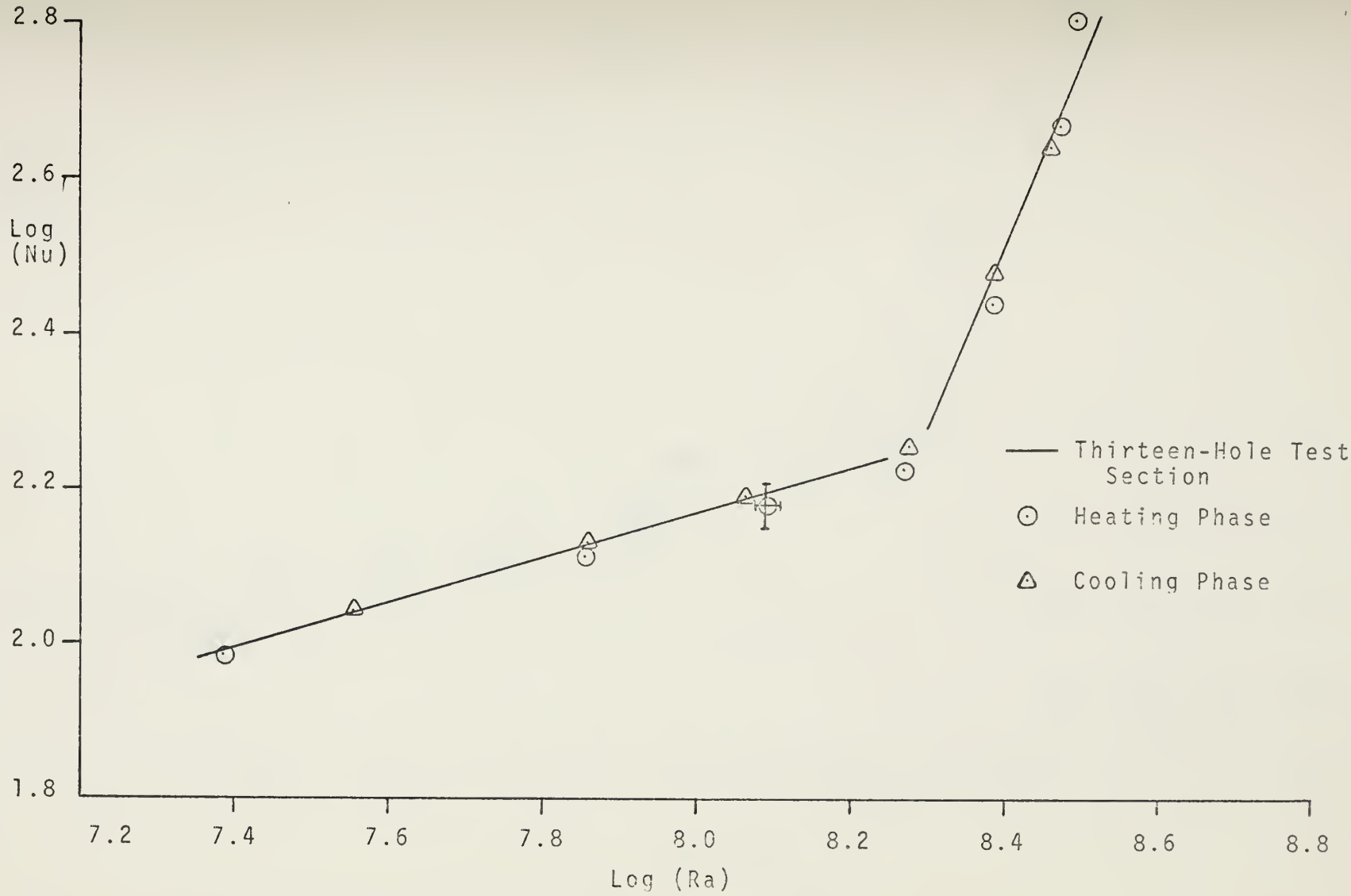

Figure 15. Results for Thirteen-Hole Test Section Based on Rayleigh Number.

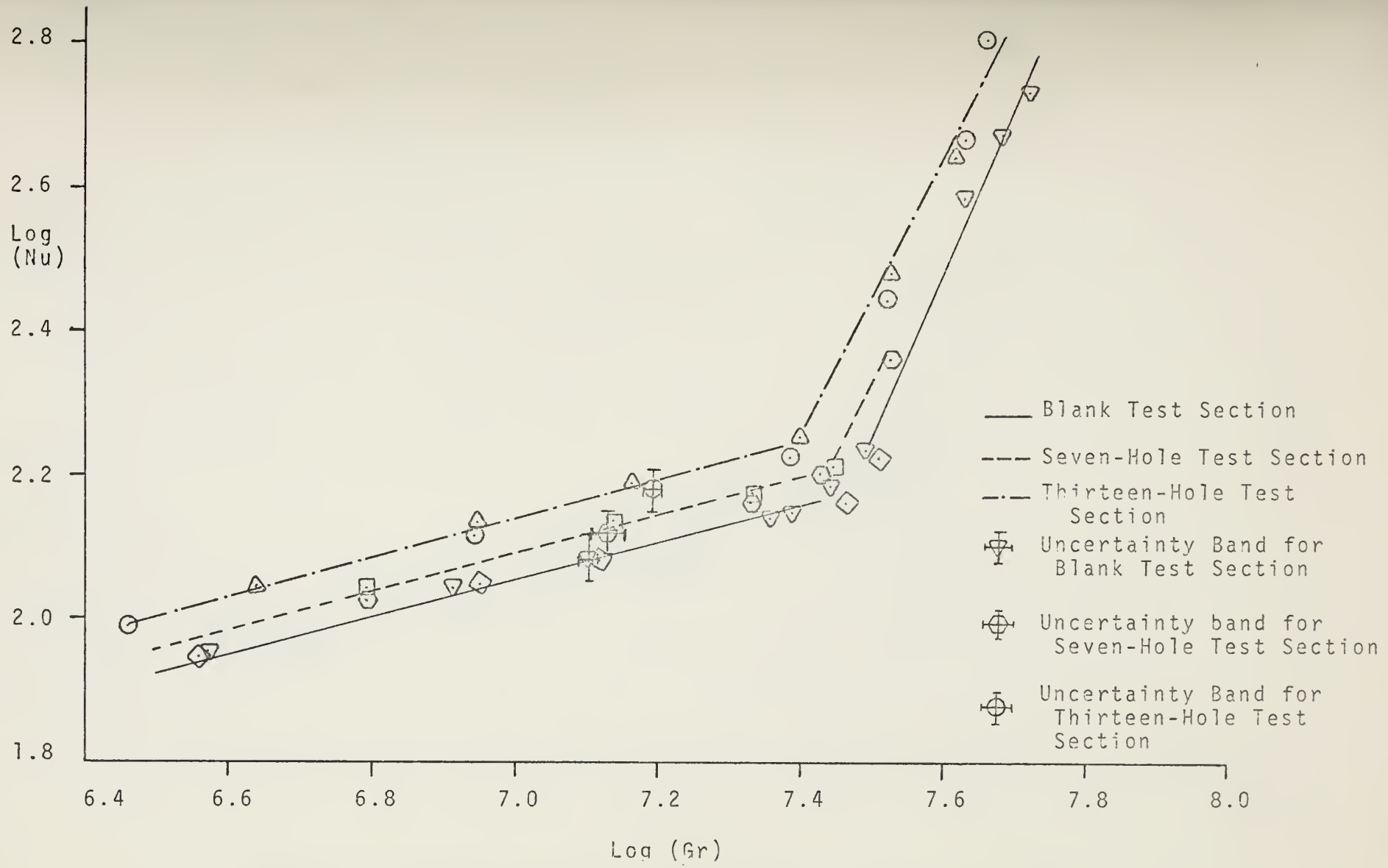

Figure 16. Correlation of Results Based on Grashof Number.

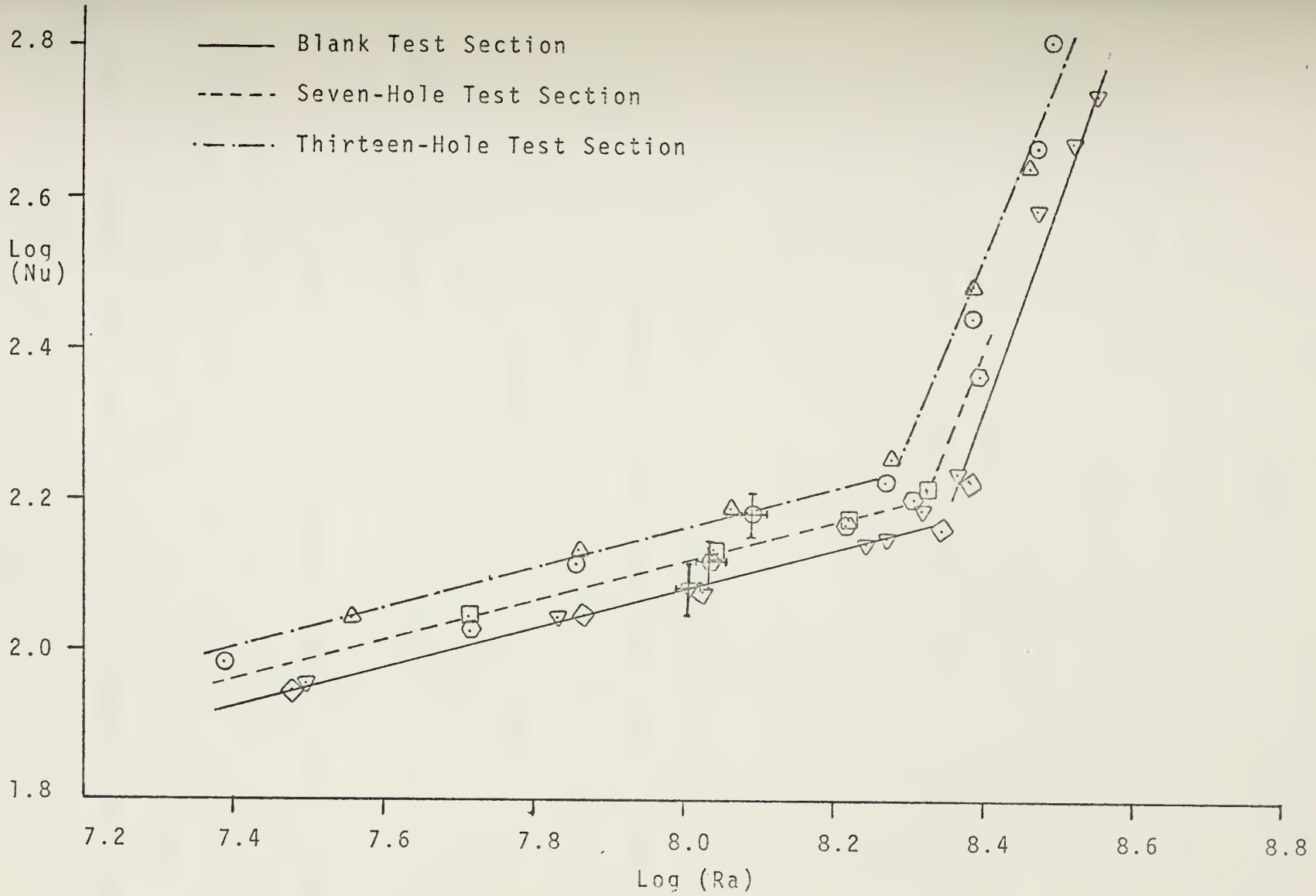

Figure 17. Correlation of Results Based on Rayleigh Number.

V. CONCLUSION

The results of this experimental work lead to the following conclusions:

1. The artificial cylindrical drilled cavities affect the natural convection by increasing the heat transfer coefficient of fluid as shown in Figure 16 for the log-log plot of Nusselt number versus Grashof number and Figure 17 for the log-log plot of Nusselt number versus Rayleigh number.

2. The correlation results for this experimental work (the horizontal circular heated disk in cylindrical enclosure) are:

$$Nu = 0.48(Ra)^{.30}, \text{ for blank test section.}$$

$$Nu = 0.53(Ra)^{.30}, \text{ for seven-hole test section.}$$

$$Nu = 0.57(Ra)^{.30}, \text{ for thirteen-hole test section.}$$

All of these correlations were in the range of Rayleigh number from $30x10^6$ to $180x10^6$. For the value of Rayleigh number from $200x10^6$ to $350x10^6$ the slope is increased as seen in Figures 10-17.

3. The log-log plot of Nusselt number versus Grashof number and Nusselt number versus Rayleigh number shows that the curves were straight lines and had nearly the same slope in the range of Grashof number from $3x10^6$ to $20x10^6$ and Rayleigh number from $30x10^6$ to $180x10^6$. Between the range of Rayleigh number from $180x10^6$ to $200x10^6$ the slope started to

change for each curve, and then the curves were straight lines again for Rayleigh number greater than 200×10^6 as shown in Figures 16 and 17.

4. Determining the surface temperature by the method of linear extrapolation as shown in Figure 18, gives the results within an error of 0.5°F. This is insufficient because the results show that if the surface temperature is changed by only .2-.3°F, the value of Nusselt number varies by about $\pm$ 10% in the lower power input setting. This made the log of Nusselt number change by about $\pm$12%.

APPENDIX A

THERMOCOUPLE CALIBRATION PROCEDURE

The accurate determination of the test section and fluid temperatures was a major part of this experiment since all the results and discussion are based on these temperatures. For this reason, precise calibration of the sheathed and bulk temperature thermocouples was necessary. When the calibration was accomplished all the wiring and recording instruments that would be used in the experiment were not changed.

A Rosemount Calibration System, with a constant temperature oil bath, was used for the calibration. The ice junction thermocouple which was sealed in a glass tube filled with oil was placed in the electronic ice point reference junction. The four sheathed thermocouples and nine bulk temperature thermocouples were suspended several inches into the oil bath. A Platinum Resistance Thermometer in conjunction with a commutation bridge was used as a standard. The calibration was conducted over a range from 80°F to 220°F and a maximum error for the thermometer for this range of temperature was 0.004 millivolt.

The results of these thermocouples reading compared with standard thermocouple tables. The deviation from the table values ranged from +.004 to +.016 millivolt for sheathed thermocouple, and the deviation from table value ranged from +.006 to +.016 millivolt for bulk temperature thermocouples.

Since all the deviation is in the position range the decision was made to use the reading value and subtract the average difference from the table value. The values of uncertainty for sheathed thermocouples was 0.2°F and uncertainty of 0.2°F for the bulk temperature.

APPENDIX B

SAMPLE CALCULATIONS

For Thirteen-Hole Test Section:

Input Power = 3.382 watts
(Data recorded 6 October 1975)

A. DETERMINATION OF THE SURFACE TEMPERATURE

A graphical method was used to determine the surface temperature. For each input setting a plot of the temperature versus the thermocouple distance from the surface, as shown in Figure 18, was made using all four reading of sheathed thermocouples. The plots were linear and the surface temperature could be obtained within an error of 0.5°F.

B. CALCULATION OF THE PRANDLE NUMBER

From the definition:

$$Pr = \frac{\nu}{\alpha} = \frac{\mu}{\rho} \cdot \rho \frac{C_p}{k_f} = \mu \frac{C_p}{k_f} \qquad (10)$$

where fluid properties were evaluated at film temperature.

$$[T_f = \frac{T_S + T_b}{2} = 86.6°F]$$

Fluid properties at T_f = 86.6°F [data from Table II from Thermophysical Properties of Refrigerants [Ref. 4]].

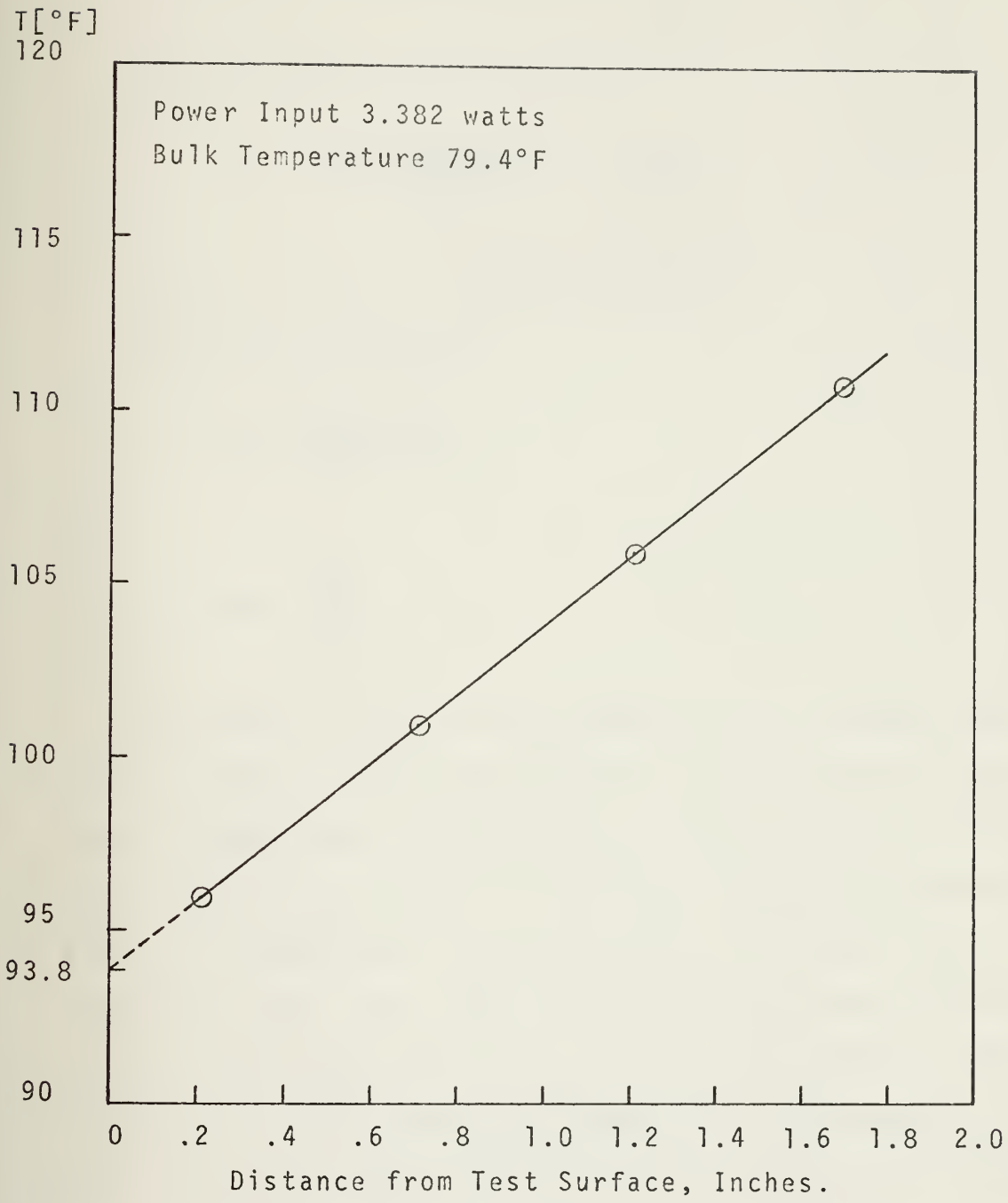

Figure 18. Determination of Surface Temperature.

$$\mu = 1.519 \text{ lb}_m/\text{ft-hr}$$

$$k_f = .04277 \text{ BTU/hr-ft-°F}$$

$$C_p = .230 \text{ BTU/lb}_m\text{-°F}$$

Using equation (10), we have

$$Pr = \frac{(1.519)(.230)}{.04277} = 8.1686$$

C. CALCULATION OF THE NUSSELT NUMBER

Using the equations:

$$h = \frac{K_{SS}(\delta T_2)}{(\delta x)(\delta T_1)} \qquad (5)$$

and

$$Nu = \frac{hD}{k_f} \qquad (6)$$

The value of K_{SS} was determined for an average temperature of cylinder over the length δx. The average of the two nearest temperatures to the test surface in the stainless steel cylinder were used. The value of K_{SS} was obtained from a plot of temperature versus K_{SS} based on values from Touloukian [Ref. 5]. Again fluid properties were evaluated at the film temperature using the data from Table II and Table 13 from Thermophysical Properties of Refrigerant 113 [Ref. 4] and the following data were obtained for 3.382 watts.

T_2 = 105.9°F

T_3 = 100.9°F

K_{SS} = 8.926 BTU/hr-ft-°F

D = .07467 ft.

δT_1 = 14.6°F

δT_2 = 5.00°F

δx = .04175 ft.

ρ = 96.9 $lb_m/ft.^3$

The value of β were calculated by definition from the thermo-dynamic properties [Ref. 6]

$$\beta = -\frac{1}{\rho}\frac{d\rho}{dT}\Big|_\rho = -\frac{1}{\rho}\left(\frac{\rho_1-\rho_0}{T_1-T_0}\right)\Big|_\rho$$

where

$$\rho = \frac{\rho_1+\rho_0}{2}$$

T_1-T_0 = Temperature difference of the given value ρ_1 and ρ_0. From Table 13 is 2°F.

For this run, we have

$$\beta = 8.668\times10^{-4}\ \frac{1}{°F}$$

Using equation (5) and (6), the Nusselt number is obtained:

$$h = \frac{8.926(5.)}{.04175(14.4)} = 74.235\ BTU/hr/ft^2/°F$$

$$Nu = \frac{74.235(0.07467)}{0.04277} = 129.597$$

D. CALCULATION OF THE GRASHOF NUMBER

Using equation:

$$Gr = (g\beta/\nu^2)\, D^3\, \delta T_1 \qquad (8)$$

The Grashof number is obtained

$$Gr = \frac{32.174 \times 8.668\times10^{-4}}{\left(\frac{1.519}{96.9\times3600}\right)^2} \quad (0.07467)^3(14.4)$$

$$= 8.817\times10^{6}$$

E. CALCULATION OF THE RAYLEIGH NUMBER

Using equation:

$$Ra = Gr \cdot Pr \qquad (9)$$

Thus

$$Ra = (8.817\times10^{6})\ (8.1686)$$

$$= 7.202\times10^{7}$$

APPENDIX C

UNCERTAINTY ANALYSIS

In this experimental work the method proposed by Kline and McClintock [Ref. 7] was used to obtain the uncertainties. Several assumptions and approximations had to be made in order to develop a reasonable estimate of the uncertainties for each variable. The following table is summary of these quantities.

TABLE IV

Uncertainty of Variables

Variable	Basis for Value	Uncertainty (U)
Cp	assumption based on table values [Ref. 4]	5×10^{-4} BTU/lb_m-°F
D	accuracy of measurement	2×10^{-4} ft.
k_f	assumption based on table values [Ref. 4]	1×10^{-3} BTU/hr-ft-°F
K_{SS}	assumption based on table values [Ref. 5]	5%
T_S	based on scale of graphical method	0.5°F
T_b	thermocouple calibration	0.2°F
T_2, T_3	thermocouple calibration	0.2°F
δx	accuracy of measurement	4.2×10^{-4} ft.
β	assumption based on table values [Ref. 4]	1×10^{-5} 1/°R
ρ	assumption based on table values [Ref. 4]	1×10^{-2} $lb_m/ft.^3$
μ	assumption based on table values [Ref. 4]	2×10^{-3} lb_m/ft-hr

The method that proposed by Kline and McClintock [Ref. 7] for determining the uncertainty values is the second-power equation.

Uncertainties in the temperature differences δT_1 and δT_2 were calculated from

$$U_{\delta T_1} = U_{T_S - T_b} = [(U_{T_S})^2 + (U_{T_b})^2]^{\frac{1}{2}}$$

$$= [(0.5)^2 + (0.2)^2]^{\frac{1}{2}} = .538°F$$

and

$$U_{\delta T_2} = U_{T_2 - T_3} = [(U_{T_2})^2 + (U_{T_3})^2]^{\frac{1}{2}}$$

$$= [(0.2)^2 + (0.2)^2]^{\frac{1}{2}} = .283°F$$

Where U_{T_S} = uncertainty in T_S

U_{T_b} = uncertainty in T_b

same as U_{T_2}, U_{T_3} = uncertainty in T_2 and T_3 respectively.

Uncertainty in the convective heat transfer coefficient (h) was determined by using

$$\frac{U_h}{h} = \left[\left(\frac{U_{K_{SS}}}{K_{SS}}\right)^2 + \left(\frac{U_{\delta T_2}}{\delta T_2}\right)^2 + \left(\frac{U_{\delta x}}{\delta x}\right)^2 + \left(\frac{U_{\delta T_1}}{\delta T_1}\right)^2\right]^{\frac{1}{2}} \qquad (11)$$

All values of uncertainties are obtained from Table IV.

The Nusselt number is defined as

$$Nu = \frac{hD}{k_f} \tag{12}$$

and used of the second power equation for uncertainty in this number becomes

$$U_{Nu} = \left[\left(\frac{U_h}{h}\right)^2 + \left(\frac{U_D}{D}\right)^2 + \left(\frac{U_{k_f}}{k_f}\right)^2\right]^{\frac{1}{2}} \tag{13}$$

It can be shown that the values of $\left(\frac{U_D}{D}\right)^2$ and $\frac{U_{k_f}}{k_f}$ are very small and can be neglected. Therefore,

$$\frac{U_{Nu}}{Nu} = \frac{U_h}{h} \tag{14}$$

To find the uncertainty of the Grashof number use this relation:

$$Gr = (g\beta/\nu^2)\, D^3\, \delta T_1$$

so

$$\frac{U_{Gr}}{Gr} = \left[\left(\frac{U_\rho}{\beta}\right)^2 + \left(2\frac{U}{\rho}\rho\right)^2 + \left(2\frac{U_\mu}{\mu}\right)^2 + \left(3\frac{U}{D}D\right)^2 + \left(\frac{U_{\delta T_1}}{\delta T_1}\right)^2\right]^{\frac{1}{2}} \tag{15}$$

The values of U are found from Table IV.

And by definition for Prandtl number is:

$$Pr = \frac{\mu C_p}{k_f}$$

so

$$\frac{U_{Pr}}{Pr} = \left[\left(\frac{U_{\mu}}{\mu}\right)^2 + \left(\frac{U_{Cp}}{Cp}\right)^2 + \left(\frac{U_{k_f}}{k_f}\right)^2\right]^{\frac{1}{2}} \qquad (16)$$

against all the values of U are found from Table IV. Find the uncertainty value for the Rayleigh number,

where

$$Ra = Gr \cdot Pr$$

$$\frac{U_{Ra}}{Ra} = \left[\left(\frac{U_{Gr}}{Gr}\right)^2 + \left(\frac{U_{Pr}}{Pr}\right)^2\right]^{\frac{1}{2}} \qquad (17)$$

A summary results of this analysis are given for each run in Table V for blank test section and in Table VI for seven-hole test section and for thirteen-hole in Table VII.

TABLE V

Uncertainties in the Experiment (Blank)

Power Input (Watts)	Percent Uncertainty		
	Nusselt Number	Grashof Number	Rayleigh Number
1.167	20.09	8.40	8.70
3.140	9.12	4.04	4.67
4.503	7.33	3.10	3.90
7.640	5.90	2.20	3.30
8.440	5.80	2.16	3.23
9.536	5.69	2.08	3.19
11.330	5.55	1.99	3.14
24.500	5.30	1.89	3.13
29.655	5.28	1.83	3.10
34.735	5.26	1.80	3.10

TABLE VI

Uncertainties in the Experiment (Seven-Hole)

Power Input (Watts)	Percent Uncertainty		
	Nusselt Number	Grashof Number	Rayleigh Number
2.429	11.30	5.06	5.64
5.300	6.80	2.90	3.74
7.791	5.98	2.32	3.33
10.060	5.66	2.09	3.19
14.970	5.42	1.95	3.12

TABLE VII

Uncertainties in the Experiment (Thirteen-Hole)

Power Input (Watts)	Percent Uncertainty		
	Nusselt Number	Grashof Number	Rayleigh Number
1.167	23.20	10.26	11.09
3.382	8.48	4.00	4.64
5.758	6.42	2.75	3.64
9.176	5.68	2.15	3.22
16.300	5.39	1.98	3.14
26.280	5.31	1.90	3.13
34. 85	5.29	1.91	3.16

BIBLIOGRAPHY

1. Duncan, D.S., "Natural Convection Heat Transfer From a Horizontal Disk in a Cylindrical Enclosure," M.S. Thesis, Naval Postgraduate School, Monterey, California, 1971.

2. Le Vinh Hiep, "The Influence of Drilled Cavities On Natural Convection Heat Transfer From a Horizontal Surface," M.S. Thesis, Naval Postgraduate School, Monterey, California, June 1975.

3. O'Conner, J.M., "Natural Convection Flow Visualization and Heat Transfer From a Horizontal Circular Disk," M.S. Thesis, Naval Postgraduate School, Monterey, California, June 1974.

4. Thermophysical Properties of Refrigerants, 2nd ed., ASHRAE, 1973.

5. Touloukian and DeHitt, Thermophysical Properties of Matter, V. 1, 1970.

6. Streeter, V.L., Fluid Mechanics, 5th ed., McGraw-Hill, 1971.

7. Kline, S.J. and McClintock, F.A., " Describing Uncertainty in Single Sample Experiments," Mechanical Engineering, V. 75, p. 3-8, January 1953.

8. Marto, P.J., Moulson, J.A., Maynard, M.D., "Nucleate Pool Boiling of Nitrogen With Different Surface Conditions," J. of Heat Transfer, V. 90, p. 437-444, November 1968.

9. Ostrach, S., " New Aspects of Natural Convection Heat Transfer," Trans. ASME, V. 75, p. 1287-1290, 1953.

10. Torrance, K.E., Orloff, L., and Rockett, J.A., "Experiments on Natural Convection in Enclosures with Localized Heating From Below," J. of Fluid Mechanics, V. 36, part 1, p. 21-23, 1969.

11. Torrance, K.E., Orloff, L., and Rockett, J.A., "Numerical Study of Natural Convection in an Enclosure With Localized Heating From Below-Creeping Flow to the Onset of Laminar Instability," J. of Fluid Mechanics, V. 36, part 1, p. 33-54, 1969.

12. Holman, J.P., Heat Transfer, 3rd ed., McGraw-Hill, 1972.

13. Knudsen, J.G. and Katz, D.L.," Fluid Dynamics and Heat Transfer," McGraw-Hill, 1958.

14. Kays, W.M., " Convection of Heat and Mass Transfer," McGraw-Hill, 1958.

INITIAL DISTRIBUTION LIST

		No. Copies
1.	Defense Documentation Center Cameron Station Alexandria, VA 22314	2
2.	Library, Code 0202 Naval Postgraduate School Monterey, CA 93940	2
3.	Department Chairman, Code 59 Department of Mechanical Engineering Naval Postgraduate School Monterey, CA 93940	2
4.	Assoc. Professor M. D. Kelleher Department of Mechanical Engineering Naval Postgraduate School Monterey, CA 93940	2
5.	First Lieutenent Apichart Penkitti, REA Military Research and Development Center Bangkok, Thailand	2

Thesis
P3296
c.1

Penkitti
The influence of artificial cavities on natural convection heat transfer from a horizontal surface.

104081